

# Assessing variable activity for Bayesian regression trees

Akira Horiguchi<sup>\*1</sup>, Matthew T. Pratola<sup>1</sup>, and Thomas J. Santner<sup>1</sup>

<sup>1</sup>*Department of Statistics  
The Ohio State University  
Cockins Hall  
1958 Neil Ave.  
Columbus, OH 43210*

September 9, 2022

## Abstract

Bayesian Additive Regression Trees (BART) are non-parametric models that can capture complex exogenous variable effects. In any regression problem, it is often of interest to learn which variables are most active. Variable activity in BART is usually measured by counting the number of times a tree splits for each variable. Such one-way counts have the advantage of fast computations. Despite their convenience, one-way counts have several issues. They are statistically unjustified, cannot distinguish between main effects and interaction effects, and become inflated when measuring interaction effects. An alternative method well-established in the literature is Sobol' indices, a variance-based global sensitivity analysis technique. However, these indices often require Monte Carlo integration, which can be computationally expensive. This paper provides analytic expressions for Sobol' indices for BART predictors. These expressions are easy to interpret and are computationally feasible. Furthermore, we will show a fascinating connection between main-effects Sobol' indices and one-way counts. We also introduce a novel ranking method, and use this to demonstrate that the proposed indices preserve the Sobol'-based rank order of variable importance. Finally, we compare these methods using analytic test functions and the En-ROADS climate impacts simulator.

## 1 Introduction

Bayesian Additive Regression Trees (BART) have become an increasingly popular tool for complex regression problems and as emulators of expensive computer simulations (Chipman et al., 2010, 2012; Gramacy and Haaland, 2016). BART sidesteps the  $O(N^3)$  matrix decompositions required by arguably the most popular statistical regression tool, Gaussian processes (GPs) (Santner et al., 2018). These cubic matrix

---

<sup>\*</sup>Corresponding author. Email: [ahoriguchi9991@gmail.com](mailto:ahoriguchi9991@gmail.com)

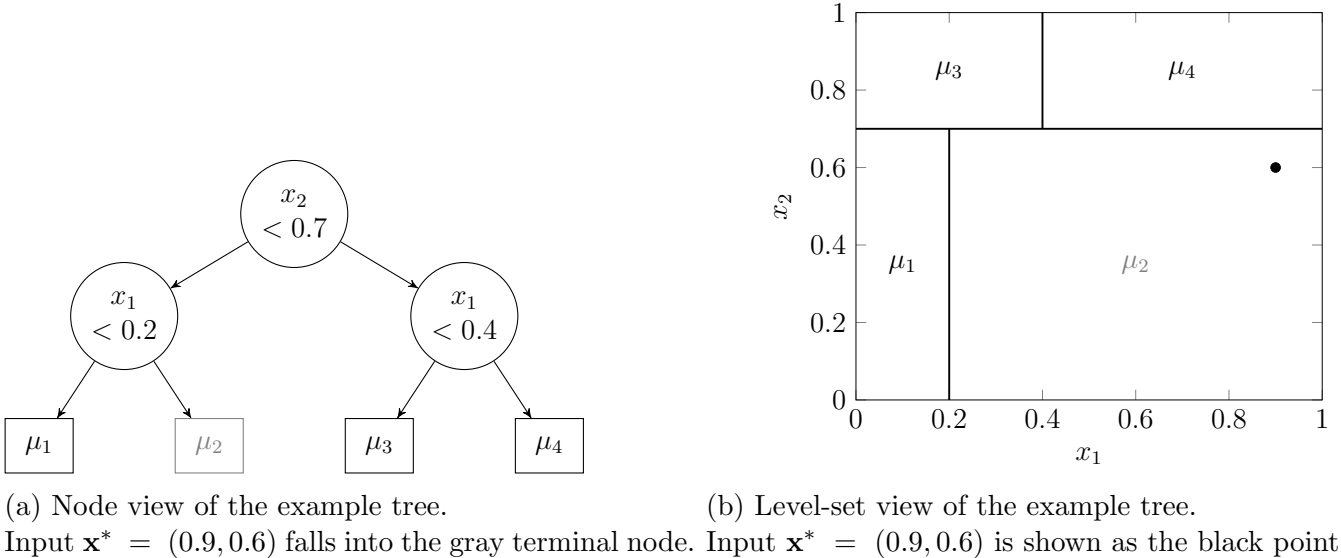


Figure 1: Two different views of the same example tree.

operations pose issues whose severity continues to grow in the era of big data. BART, like GPs, can capture complex exogenous variable effects without having to specify their functional forms.

To assess the activity of these exogenous input variables, BART offers a variable count heuristic proposed by Chipman et al. (2010), which comes nearly for free once a BART model is fit. This method counts the number of times a variable is included in BART’s trees as a split variable. For example, the tree in Figure 1a splits on  $x_1$  twice and on  $x_2$  once. Using this heuristic, input  $x_1$  would be considered to be twice as active as input  $x_2$ . The idea is that if many nodes in BART’s trees split on a variable, then that variable is deemed important in predicting the response. To this day, count-based methods remain the most popular way of assessing input activity in BART. For example, Bleich et al. (2014) also rely on these posterior inclusion proportions in their proposed variable selection methods.

But as Liu et al. (2018) note, one-way counts are not theoretically well-understood. Furthermore, their ability to adequately capture even the order of input importance is suspect. Figure 2 shows the variable counts of 1,000 posterior samples from a BART model trained in data generated from the function  $f(\mathbf{x}) = (x_1 - 0.5)(x_2 - 0.5) + 0.5(x_3 - 0.5)$  on the unit hypercube  $[0, 1]^3$ . Marginally, variables  $x_1$  and  $x_2$  have zero effect on  $f(\cdot)$ , which makes variable  $x_3$  marginally the most important input. But the variable counts in Figure 2 show  $x_1$  and  $x_2$  to be more active than  $x_3$ . Thus, the individual marginal counts seem to conflate the interaction effect between  $x_1$  and  $x_2$  with their marginal effects.

To better assess input activity, we may instead use the variance-based global sensitivity analysis method introduced by Sobol’ (1993). He showed that if  $f(\mathbf{x})$  is a real-valued, square-integrable function on  $[0, 1]^p$  then  $f(\mathbf{x})$  can be decomposed into a sum

$$f(\mathbf{x}) = f_0 + \sum_{i=1}^d f_i(x_i) + \sum_{i=1}^d \sum_{j < i}^d f_{ij}(x_i, x_j) + \cdots + f_{1,2,\dots,d}(x_1, x_2, \dots, x_d),$$

where each summand depends on a subset of  $\mathbf{x}$ . Assume that the relative frequency with which the inputs of  $f(\mathbf{x})$  occur can be modeled by  $\mathbf{X} = (X_1, X_2, \dots, X_d)$  where  $X_1, \dots, X_d \stackrel{iid}{\sim} U(0, 1)$ . Then if the variance

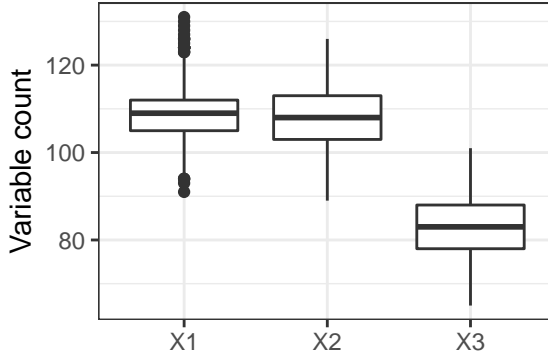


Figure 2: One-way variable counts of 1,000 posterior samples from a BART ensemble trained in data generated from the function  $f(\mathbf{x}) = (x_1 - 0.5)(x_2 - 0.5) + 0.5(x_3 - 0.5)$  on the unit hypercube  $[0, 1]^3$ .

of the  $i$ th term in the Sobol' expansion which depends on  $x_i$  is large, then  $x_i$  is deemed important in predicting the response. Computing these variances and expectations requires Monte Carlo integration when  $f(\mathbf{x})$  is not known in closed form, and hence becomes untractable as the number of inputs increases.

Our primary contribution is to use Sobol' indices for BART model-based input activity. We derive analytic expressions that can be computed exactly and do not require expensive Monte Carlo integration. We furthermore establish a connection between main-effects Sobol' indices and one-way counts. Finally, we compare the methods using analytic test functions and demonstrate that Sobol' indices applied to BART accurately capture true variable effects while remaining computationally attractive and easy to interpret. To perform this comparison, we consider both the estimation of the Sobol' indices and evaluate the order-preserving sequence of active variables using a proposed novel rank-order statistic.

The rest of the paper is organized as follows. In Section 2, we review BART. In Section 3, we derive Sobol' indices for BART and establish a connection between main-effects Sobol' indices and one-way counts. In Section 4, we provide computational details and introduce our rank-order statistic. In Section 5, we perform simulation studies and apply Sobol' indices to a BART-based emulator of the En-ROADS climate simulator. In Section 6, we conclude the paper with a discussion. Proofs of stated theorems can be found in the Appendix.

## 2 Review of BART

We wish to make inference on an unknown function  $f: D \rightarrow \mathbb{R}$ , where domain  $D$  is a  $p$ -dimensional subset of  $\mathbb{R}^p$ . We will assume for the rest of the text that domain  $D$  is a bounded hyperrectangle, i.e.  $D = \prod_{j=1}^p I_D^j = \prod_{j=1}^p [a_D^j, b_D^j]$ , where  $I_D^j$  is the  $j$ th marginal interval of  $D$  for  $j = 1, \dots, p$ . We observe the data  $\mathcal{D} := \{(y(\mathbf{x}_i), \mathbf{x}_i)\}_{i=1, \dots, n}$ , where each observation  $y(\mathbf{x})$ , based on predictor  $\mathbf{x} = (x_1, \dots, x_p) \in D$ , is assumed to be a realization of the random variable

$$Y(\mathbf{x}) = f(\mathbf{x}) + \epsilon, \quad (1)$$

where  $\epsilon \stackrel{iid}{\sim} N(0, \sigma^2)$ .

To make inference about the unknown function  $f(\cdot)$ , we approximate it by a sum of  $m$  regression trees.

That is, we make the approximation

$$f(\mathbf{x}) \approx \sum_{t=1}^m g(\mathbf{x}; \mathcal{T}_t, \mathcal{M}_t), \quad (2)$$

where each  $g(\cdot; \mathcal{T}_t, \mathcal{M}_t) : D \rightarrow \mathbb{R}$  denotes a regression tree function and the parameters  $\{\mathcal{T}_t, \mathcal{M}_t\}_{t=1}^m$  are given a prior distribution in BART's hierarchical Bayesian model structure. Each  $g(\cdot; \mathcal{T}_t, \mathcal{M}_t)$  contributes a small portion to the total approximation of  $f(\cdot)$ . Hence, the expected response  $\mathbb{E}[Y(\mathbf{x}) \mid \{(\mathcal{T}_t, \mathcal{M}_t)\}_{t=1}^m]$  at a given input  $\mathbf{x}$  is the sum of each of the contributions  $g(\mathbf{x}; \mathcal{T}_t, \mathcal{M}_t)$ . The model in Equation 2 is called a sum-of-trees model.

## 2.1 Single-tree model

To explain the sum-of-trees model, we will first set the number of trees  $m = 1$  and describe the notation of the resulting single-tree model.

The single-tree model is the Bayesian implementation of the Classification and Regression Tree (CART) model as proposed in Chipman et al. (1998). CART can be used for classification, but we assume for the paper that it is being applied to the regression setting as described in Equation 1. The CART model provides a prediction of  $f(\mathbf{x})$  at input point  $\mathbf{x}$  given observed data  $\mathcal{D}$ . CART partitions the input space and fits a constant mean model in each subregion to form the predictions. CART constructs the partition via a binary tree structure. To form the partitions, each internal node contains a boolean split rule. Starting at the root node, if an input point  $\mathbf{x}$  satisfies the split rule, it will travel to the node's left child; otherwise  $\mathbf{x}$  will travel to the right child. The input point  $\mathbf{x}$  will continue to traverse through the tree in this way until it reaches a terminal node. This terminal node's parameter is the predicted value of  $f(x)$ .

Figure 1 shows an illustrative example. Suppose the tree in Figure 1a is used in a single-tree model to predict an output value for input  $\mathbf{x}^* = (x_1^*, x_2^*) = (0.9, 0.6)$ , where the input space  $D$  is the closed unit-square  $[0, 1]^2$ . Starting at the root node in Figure 1a, we see that  $\mathbf{x}^*$  satisfies this split rule (i.e.  $x_2^* < 0.7$ ), which moves  $\mathbf{x}^*$  to the left child. We then see that  $\mathbf{x}^*$  satisfies this split rule (i.e.  $x_1^* \geq 0.8$ ), which moves  $\mathbf{x}^*$  to the right child, which turns out to be a terminal node. Because we are using a single-tree model (i.e. there is exactly  $m = 1$  tree), this mean parameter  $\mu_2$  becomes the predicted value for input  $\mathbf{x}^*$ . Figure 1b shows the corresponding hyperrectangle view of the tree.

A tree's parameters can now be organized in the following manner. Let  $\mathcal{T}$  denote the set of parameters associated with the tree's split rules (i.e. the split variable and cutpoint for each internal node) and topology. Let  $\mathcal{M}$  denote the set  $\{\mu_k\}$  of parameters associated with the tree's terminal nodes. The single-tree model is thus  $f(\cdot) \approx g(\cdot; \mathcal{T}, \mathcal{M})$ , where  $f(\cdot)$ , defined in Equation 1, is the mean of the observed process. Here, we think of  $g(\cdot; \mathcal{T}, \mathcal{M})$  being a function that assigns a value  $\mu_k$  to input  $\mathbf{x}$  according to the parameters in  $\mathcal{T}$  and  $\mathcal{M}$ . Let  $\mathbf{R}_k \subset D$  denote the hyperrectangle associated with terminal node  $\eta_k$  of tree  $T$ . Then,

$$g(\cdot; \mathcal{T}, \mathcal{M}) = \sum_{k=1}^{|\mathcal{M}|} \mu_k \mathbf{1}_{\mathbf{R}_k}(\cdot). \quad (3)$$

We may further decompose each hyperrectangle  $\mathbf{R}_k$  into the Cartesian product of its  $p$  marginal intervals  $I_k^1, \dots, I_k^p$  and hence write  $\mathbf{1}_{\mathbf{R}_k}(\mathbf{x}) = \prod_{i=1}^p \mathbf{1}_{I_k^i}(x_i)$ .

## 2.2 Sum-of-trees model

Now consider the sum-of-trees model in Equation 2 for  $m > 1$ . If the parameter sets  $\{(\mathcal{T}_t, \mathcal{M}_t)\}_{t=1}^m$  have been established, we will let the function

$$\mathcal{E}(\cdot) := \sum_{t=1}^m g(\cdot; \mathcal{T}_t, \mathcal{M}_t) = \sum_{t=1}^m \sum_{k=1}^{|\mathcal{M}_t|} \mu_{tk} \mathbf{1}_{\mathbf{R}_{tk}}(\cdot) \quad (4)$$

denote the sum-of-trees approximation in Equation 2. To streamline notation, we will refer to  $\mathcal{E}$  as both the function  $\mathcal{E}(\cdot)$  and as the collection  $\{(\mathcal{T}_t, \mathcal{M}_t)\}_{t=1}^m$ . Thus, we write  $(\mathcal{T}, \mathcal{M}) \in \mathcal{E}$  if  $(\mathcal{T}, \mathcal{M}) = (\mathcal{T}_t, \mathcal{M}_t)$  for some  $t = 1, \dots, m$ .

## 2.3 Bayesian tree models

The sum-of-trees model is specified by the parameters  $\{(\mathcal{T}_t, \mathcal{M}_t)\}_{t=1}^m$  and  $\sigma^2$ . Hence, a trained BART model will sample from the posterior distribution

$$\pi(\Theta \mid \mathcal{D}) \propto L(\Theta \mid \mathcal{D}) \pi(\Theta), \quad (5)$$

where  $\Theta = \{(\mathcal{T}_1, \mathcal{M}_1), (\mathcal{T}_2, \mathcal{M}_2), \dots, (\mathcal{T}_m, \mathcal{M}_m), \sigma^2\}$  are the parameters,  $\mathcal{D}$  is the observed data,

$$L(\Theta \mid \mathcal{D}) \propto \sigma^{-n} \exp \left( -\frac{1}{2\sigma^2} \sum_{i=1}^n \left( y(\mathbf{x}_i) - \sum_{t=1}^m g(\mathbf{x}_i; \mathcal{T}_t, \mathcal{M}_t) \right)^2 \right)$$

is the likelihood, and  $\pi(\Theta)$  is the prior.

Chipman et al. (2010) specify the full prior  $\pi(\Theta)$  by constraining it to satisfy independence conditions

$$\pi(\Theta) = \left[ \prod_{t=1}^m \pi(\mathcal{M}_t \mid \mathcal{T}_t) \pi(\mathcal{T}_t) \right] \pi(\sigma^2), \quad (6)$$

and

$$\pi(\mathcal{M}_t \mid \mathcal{T}_t) = \prod_{k=1}^{|\mathcal{M}_t|} \pi(\mu_{tk} \mid \mathcal{T}_t) \quad (7)$$

for all  $t = 1, \dots, m$ . In Equation 6, the parameter sets  $(\mathcal{T}_t, \mathcal{M}_t)$  and  $\sigma^2$  are constrained to be mutually independent. In Equation 7, the terminal node parameters of every tree are constrained to be independent. These independence conditions simplify the problem of specifying the full prior  $\pi(\Theta)$  to specifying only the priors  $\pi(\mathcal{T}_t)$ ,  $\pi(\mu_{tk} \mid \mathcal{T}_t)$ , and  $\pi(\sigma^2)$ . Forcing the priors  $\pi(\mathcal{T}_t)$  and  $\pi(\mu_{tk} \mid \mathcal{T}_t)$  to be identical for all  $k = 1, \dots, |\mathcal{M}_t|$  and  $t = 1, \dots, m$  further simplifies the prior specification problem. Furthermore, Chipman et al. (1998) choose the three prior forms to simplify analysis and computation by taking advantage of known conjugacy pairs. In particular, they choose the  $\pi(\mu_{tk} \mid \mathcal{T}_t)$  prior to be a conjugate Normal distribution. To configure the priors, Chipman et al. (2010) recommend automatically specifying the relevant hyperparameters using data-driven methods.

The posterior in Equation 5 can thus be sampled using the following Gibbs sampler:

1. Draw  $\{(\mathcal{T}_t, \mathcal{M}_t)\}_{t=1}^m \mid \sigma^2, \mathcal{D}$ .

2. Draw  $\sigma^2 \mid \{(\mathcal{T}_t, \mathcal{M}_t)\}_{t=1}^m, \mathcal{D}$ .

For Step 2, we can draw  $\sigma^2 \mid \{(\mathcal{T}_t, \mathcal{M}_t)\}_{t=1}^m, \mathcal{D}$  by performing a simple conjugate Gibbs step. Step 1 itself will also be a Gibbs sampler that relies on being able to sample from the conditional distribution

$$\pi(\mathcal{T}_t, \mathcal{M}_t \mid \{(\mathcal{T}_\tau, \mathcal{M}_\tau)\}_{\tau \neq t}, \sigma^2, \mathcal{D}) \quad (8)$$

for all  $t = 1, \dots, m$ . To sample from this conditional distribution, we simplify the likelihood by noting

$$L(\Theta \mid \mathcal{D}) \propto \sigma^{-n} \exp \left( -\frac{1}{2\sigma^2} \sum_{i=1}^n \left( r_t(\mathbf{x}_i) - g(\mathbf{x}_i; \mathcal{T}_t, \mathcal{M}_t) \right)^2 \right)$$

where  $r_t(\mathbf{x}_i) := y(\mathbf{x}_i) - \sum_{\tau \neq t} g(\mathbf{x}_i; \mathcal{T}_\tau, \mathcal{M}_\tau)$ . Therefore, the conditional distribution in Equation 8 for any  $t = 1, \dots, m$  relies on  $\{(\mathcal{T}_\tau, \mathcal{M}_\tau)\}_{\tau \neq t}$  and  $\mathcal{D}$  only through  $\mathbf{R}_t = \{(r_t(\mathbf{x}_i), \mathbf{x}_i)\}_{i=1, \dots, n}$ . Hence, the conditional distribution can be expressed as  $\pi(\mathcal{T}_t, \mathcal{M}_t \mid \mathbf{R}_t, \sigma^2)$ , where  $\mathbf{R}_t$  plays the role of  $\mathcal{D}$  in the single-tree version of Step 1 of the Gibbs sampler. Each draw from the conditional distribution in Equation 8 for any  $t = 1, \dots, m$  is then reduced to two draws:

- (a) Draw  $\mathcal{T}_t \mid \sigma^2, \mathbf{R}_t$ .
- (b) Draw  $\mathcal{M}_t \mid \mathcal{T}_t, \sigma^2, \mathbf{R}_t$ .

### 3 Sobol' indices

In Section 1, we introduced the idea from Sobol' (1993) that the variance of any real-valued function defined on and square-integrable in a unit-hypercube domain can be decomposed into a sum of variance terms. The original results from Sobol' (1993) can in fact be extended so that instead of assuming that the random variables  $X_1, X_2, \dots, X_p \stackrel{iid}{\sim} U(0, 1)$ , any continuous and mutually uncorrelated  $X_1, X_2, \dots, X_p$  with finite interval supports can be used. Thus, using Equation 4, we can decompose the variance of a BART ensemble function into a sum of terms attributed to single inputs or to interactions between sets of inputs.

In order to develop our BART-based Sobol' indices, we will require the following assumptions:

- A.1**  $X_1, \dots, X_p$  are mutually uncorrelated;
- A.2**  $X_i$ 's density  $\pi_i$  is positive almost everywhere on the domain's  $i$ th margin;
- A.3** No two internal nodes of the BART ensemble  $\mathcal{E}$  have the same split rule;
- A.4** Conditional on parameter sets  $\{(\mathcal{T}_t, \mathcal{M}_t)\}_{t=1}^m$ ,  $\mathcal{E}(\mathbf{x}) = \mathcal{E}(\mathbf{x}^*)$  holds if and only if input points  $\mathbf{x}$  and  $\mathbf{x}^*$  belong to the same set of  $m$  terminal nodes.

We use conditions **A.1** and **A.2** to extend the two original results from Sobol' (1993) and to derive Sobol' indices for BART ensembles. Conditions **A.3** and **A.4** are perhaps the most unusual of the above assumptions, but we use them only when relating Sobol' indices to counts. Regarding condition **A.3**, the default number of possible cutpoint values in McCulloch et al. (2019) is 100. Therefore, there are  $100p$  possible split rules to choose from. Thus, condition **A.3** is not an unreasonable assumption to make.

Condition **A.4** follows from each  $\mu_k|\mathcal{T}$  being conditionally Normal. If inputs  $\mathbf{x}$  and  $\mathbf{x}^*$  belong to different terminal nodes in at least one of the ensemble's trees, then the probability that  $\mathcal{E}(\mathbf{x}) = \mathcal{E}(\mathbf{x}^*)$  is zero. Therefore, condition **A.4** is a reasonable assumption to make.

We can now state the desired generalized version of the variance decomposition described in Sobol' (1993). For any random vector  $\mathbf{X} = (X_1, \dots, X_d)$  that satisfies conditions **A.1** and **A.2** on  $p$ -dimensional bounded hyperrectangle domain  $D$  and for any real-valued function  $f$  square-integrable on  $D$ , the variance of  $f(\mathbf{X})$  can be decomposed into a sum of terms attributed to single inputs or to interactions between sets of inputs. That is,

$$\text{Var}_{\mathbf{X}}(f(\mathbf{X})) = \sum_{i=1}^d V_i + \sum_{i=1}^d \sum_{i < j} V_{ij} + \dots + V_{12\dots d}, \quad (9)$$

where we recursively define for each variable index set  $P \subseteq \{1, 2, \dots, d\}$

$$V_P := \text{Var}_{\mathbf{X}_P} \left( \mathbb{E}_{\mathbf{X}_{-P}}[f(\mathbf{X}) \mid \mathbf{X}_P] \right) - \sum_{Q \in 2^P \setminus \{\emptyset, P\}} V_Q. \quad (10)$$

### 3.1 Sobol' indices applied to BART

Next, we apply this variance decomposition for general  $L_2$  functions  $f(\cdot)$  to BART ensemble functions  $\mathcal{E}(\cdot)$ . Specifically, we will compute the terms in the right hand side of Equation 9 for BART ensembles.

The core terms to compute in Equation 10 are the conditional expectation  $\mathbb{E}_{\mathbf{X}_{-P}}[\mathcal{E}(\mathbf{X}) \mid \mathbf{X}_P]$  and its variance with respect to  $\mathbf{X}_P$ . By integrating both sides of Equation 4, we obtain an analytic expression for the conditional expectation:

$$\mathbb{E}_{\mathbf{X}_{-P}}[\mathcal{E}(\mathbf{X}) \mid \mathbf{X}_P] = \sum_{k \in B_{\mathcal{E}}} d_k^{-P} \mathbf{1}_{\mathbf{R}_k^P}(\mathbf{X}_P), \quad (11)$$

where the set  $B_{\mathcal{E}}$  indexes the terminal nodes of ensemble  $\mathcal{E}$ , the  $|P|$ -dimensional hyperrectangle  $\mathbf{R}_k^P$  is the projection of terminal node  $k$ 's  $p$ -dimensional hyperrectangle  $\mathbf{R}_k$  onto the dimensions in  $P$ , and  $d_k^{-P} = \mu_k \mathbb{P}_{-P}(\mathbf{R}_k^{-P})$ , where we introduce the notation  $\mathbb{P}_P(\cdot) = \mathbb{P}_{\mathbf{X}_P}(\cdot) = \mathbb{P}(\mathbf{X}_P \in \cdot)$ . Theorem 1 then provides an analytic expression for the variance of the conditional expectation.

**Theorem 1.** *For any random vector  $\mathbf{X} = (X_1, \dots, X_d)$  that satisfies conditions **A.1** and **A.2** on  $p$ -dimensional bounded hyperrectangle domain  $D$ , the variance of the conditional expectation in Equation 11 with respect to variable index set  $P$  is*

$$\text{Var}_{\mathbf{X}_P} \left( \mathbb{E}_{\mathbf{X}_{-P}}[\mathcal{E}(\mathbf{X}) \mid \mathbf{X}_P] \right) = \sum_{k \in B_{\mathcal{E}}} \sum_{l \in B_{\mathcal{E}}} d_k^{-P} d_l^{-P} C_{k,l}^P \quad (12)$$

where  $d_k^{-P} = \mu_k \mathbb{P}_{-P}(\mathbf{R}_k^{-P})$  and  $C_{k,l}^P = \mathbb{P}_P(\mathbf{R}_k^P \cap \mathbf{R}_l^P) - \mathbb{P}_P(\mathbf{R}_k^P) \mathbb{P}_P(\mathbf{R}_l^P)$ . In particular, the (unnormalized) main-effects Sobol' index  $V_i$  (i.e.  $V_P$  when  $P = \{i\}$ ) in Equation 10 then becomes

$$V_i = \sum_{k \in B_{\mathcal{E}}} \sum_{l \in B_{\mathcal{E}}} d_k^{-i} d_l^{-i} C_{k,l}^i, \quad (13)$$

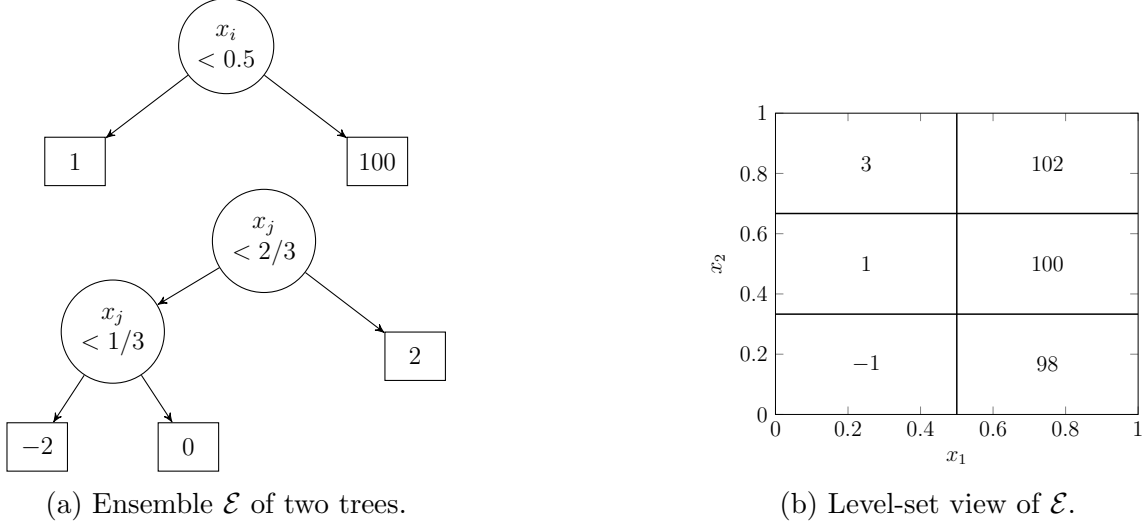


Figure 3: Two different views of the same ensemble  $\mathcal{E}$ .

where  $d_k^{-i} = \mu_k \prod_{j \neq i} \mathbb{P}_j(I_k^j)$  and  $C_{k,l}^i = \mathbb{P}_i(I_k^i \cap I_l^i) - \mathbb{P}_i(I_k^i)\mathbb{P}_i(I_l^i)$ .

### 3.2 How do counts and Sobol' indices relate?

To this day, count-based methods remain the most popular ways of assessing input activity for BART. But as Liu et al. (2018) note, they are not theoretically well-understood. We have seen in Figure 2 a scenario in which the one-way count metric not only inaccurately measures input activity in the data-generating function  $f$  but also incorrectly ranks the variables in order of importance. Chipman et al. (2010) and Bleich et al. (2014) also detail scenarios that question how accurately one-way count metric assess input activity in the data-generating function and suggest ad-hoc work-arounds, such as fitting BART with small  $m$  to get an empirically better behaved estimate of input activity. But how do counts perform when assessing input activity in the BART ensemble itself? To answer this question, we turn to the example in Figure 3a. The count metric will look at number of splits and conclude that variable  $x_j$  is twice as active than variable  $x_i$ . But if we look at the terminal node values of the ensemble, variable  $x_i$  is clearly more important than variable  $x_j$  in determining the ensemble's predicted value. If the count metric is not measuring variable importance in the ensemble, then what exactly is it measuring? Theorem 2 answers this question.

**Theorem 2.** *Fix dimension  $i$  arbitrarily and let  $\mathcal{E}$  be a BART ensemble of  $m$  regression trees that satisfies assumptions A.1, A.2, A.3, and A.4. Then the number of nodes in  $\mathcal{E}$  that split on variable  $x_i$  equals the number of jumps in the piecewise-constant function  $\mathbb{E}_{\mathbf{X}_{-i}}[\mathcal{E}(\mathbf{X}) \mid X_i = \cdot]$ .*

To see why Theorem 2 might be true, consider a BART ensemble  $\mathcal{E}_0$  with  $m$  regression trees, where each tree is simply a terminal node with one terminal node parameter. Thus, the ensemble  $\mathcal{E}_0$  predicts the same value for any input  $\mathbf{x} \in D$  and is hence a constant-mean model. Then any BART ensemble  $\mathcal{E}$  with  $m$  regression trees can be thought of as  $\mathcal{E}_0$  having undergone a sequence of birth processes. Any birth process slices a terminal node's corresponding hyperrectangle into two smaller hyperrectangles according to some split rule. If we call this split rule " $x_i < c$ ", then this slice occurs on the  $(p-1)$ -dimensional hyperplane  $x_i = c$  in  $D$ . The resulting "left" hyperrectangle gains a terminal node parameter  $\mu_{left}$  while the resulting "right" hyperrectangle gains a terminal node parameter  $\mu_{right}$ . Thus, if prior to the birth



process the piecewise-constant function  $\mathbb{E}_{\mathbf{X}_{-i}}[\mathcal{E}(\mathbf{X}) \mid X_i = \cdot]$  is constant at  $x_i = c$  (which we ensure through assumption **A.3**) and  $\mu_{left} \neq \mu_{right}$  (which is true almost surely but is also ensured through assumption **A.4**), then the birth process produces a jump in the piecewise-constant function at  $x_i = c$ . Meanwhile, the birth process does not produce a jump in any of the other piecewise-constant functions  $\mathbb{E}_{\mathbf{X}_{-j}}[\mathcal{E}(\mathbf{X}) \mid X_j = \cdot]$  (for  $j \neq i$ ). Hence, under the mentioned conditions, each birth process that splits on variable  $x_i$  increments the number of jumps in the piecewise-constant function  $\mathbb{E}_{\mathbf{X}_{-i}}[\mathcal{E}(\mathbf{X}) \mid X_i = \cdot]$  by one.

Theorem 2 also provides a link between the one-way count metric and the theoretically more well-understood main-effects Sobol' index. Under the conditions of Theorem 2, the one-way count of variable  $x_i$  is the number of jumps in the conditional expectation function  $\mathbb{E}_{\mathbf{X}_{-i}}[\mathcal{E}(\mathbf{X}) \mid X_i = \cdot]$ . Under the conditions of Theorem 1, the main-effects Sobol' index of variable  $x_i$  is the variance of the conditional expectation  $\mathbb{E}_{\mathbf{X}_{-i}}[\mathcal{E}(\mathbf{X}) \mid X_i]$ . Thus, under certain conditions, both the one-way count and the main-effects Sobol' index of variable  $x_i$  are functions of the conditional expectation function  $\mathbb{E}_{\mathbf{X}_{-i}}[\mathcal{E}(\mathbf{X}) \mid X_i = \cdot]$ .

Interestingly, the number of jumps and the variance can each be thought of as a measure of variability. Under this lens, the one-way count metric can be viewed as a more crude version of the main-effects Sobol' index. Theorem 3 describes how to “standardize” the conditional expectation function so that its variance becomes the number of jumps it has. We use the term standardize because many different conditional expectation functions can be transformed into the standardized conditional expectation function, but the standardized conditional expectation function cannot be transformed back into the original conditional expectation function.

**Theorem 3.** *Let  $\mathcal{E}$  be a BART ensemble with assumptions **A.1**, **A.2**, **A.3**, and **A.4**. Recall that for all dimensions  $i = 1, \dots, p$ , the conditional expectation function  $\mathbb{E}_{\mathbf{X}_{-i}}[\mathcal{E}(\mathbf{X}) \mid X_i = \cdot]$  is piecewise constant and hence can be written as  $\mathbb{E}_{\mathbf{X}_{-i}}[\mathcal{E}(\mathbf{X}) \mid X_i = \cdot] = \sum_{k^* \in B_{\mathcal{E}}^i} e_{k^*}^i \mathbf{1}_{I_{k^*}^i}(\cdot)$ , where  $B_{\mathcal{E}}^i$  indexes the intervals in this piecewise constant function. Consider the following transformations to this conditional expectation function:*

1. *First, center and scale the  $e_{k^*}^i$  so that its corrected sample variance equals  $|B_{\mathcal{E}}^i|$ .*
2. *Second, assign equal probability mass  $|B_{\mathcal{E}}^i|^{-1}$  to each  $I_{k^*}^i$ .*

*Then the number of jumps in this transformed conditional expectation function equals its variance.*

## 4 Computational Details

For arbitrary variable index set  $P$  and  $L^2$  function  $f$ , the expression

$$\text{Var}_{\mathbf{X}_P} \left( \mathbb{E}_{\mathbf{X}_{-P}}[f(\mathbf{X}) \mid \mathbf{X}_P] \right)$$

is at the core of all Sobol' index calculations. When  $P$  contains just a single variable, then this expression is exactly that variable's unnormalized main-effects Sobol' index. When  $P$  contains more than one variable, the unnormalized Sobol' index  $V_P$  is this expression minus the sum of all unnormalized Sobol' indices  $V_Q$ , where variable index set  $Q$  is a proper subset of  $P$ . Computing this expression for an arbitrary function  $f$  typically requires Monte Carlo approximation. But we showed in Theorem 1 that this expression can be computed exactly when  $f$  is a BART ensemble function  $\mathcal{E}$  (shown in Equation 12). Furthermore, it turns out that possibly many, if not all, of the summands in Equation 12 are zero. Theorem 4 below explains under what conditions summands vanish.



Figure 4: Two trees.

## 4.1 Unnormalized Sobol' indices

A sensible goal in sensitivity analysis is to compute all main-effects Sobol' indices. If we naïvely calculate unnormalized main-effects Sobol' index  $V_1$  for the ensemble  $\mathcal{E}$  consisting only of the two trees in Figure 4 as formulated in Equation 12, we would compute a sum of  $|B_{\mathcal{E}}|^2 = 16$  terms. But because tree  $(\mathcal{T}_2, \mathcal{M}_2)$  does not ever split on variable  $x_1$ , the conditional expectation  $\mathbb{E}[g(\mathbf{X}; \mathcal{T}_2, \mathcal{M}_2) \mid X_1 = x_1]$  is constant in  $x_1$ . Thus, the unnormalized main-effects Sobol' index

$$\begin{aligned} V_1 &= \text{Var}_{X_1}(\mathbb{E}[\mathcal{E}(\mathbf{X}) \mid X_1]) \\ &= \text{Var}_{X_1}(\mathbb{E}[g(\mathbf{X}; \mathcal{T}_1, \mathcal{M}_1) + g(\mathbf{X}; \mathcal{T}_2, \mathcal{M}_2) \mid X_1]) \\ &= \text{Var}_{X_1}(\mathbb{E}[g(\mathbf{X}; \mathcal{T}_1, \mathcal{M}_1) \mid X_1]) \end{aligned}$$

requires a sum of the square of only the two terminal nodes in tree  $(\mathcal{T}_1, \mathcal{M}_1)$ . By removing the “constant in  $x_1$ ” tree  $(\mathcal{T}_2, \mathcal{M}_2)$ , we have reduced this variance calculation from a sum of 16 terms to a sum of  $2^2 = 4$  terms. Similarly for unnormalized main-effects Sobol' index  $V_2$ , we can reduce the variance calculation from a sum of 16 terms to a sum of 4 terms. Hence, computing all unnormalized main-effects Sobol' indices reduces from a sum of  $16p \geq 32$  terms to a sum of 8 terms.

More generally, to compute Equation 12 for arbitrary variable index set  $P$ , we may remove any tree that does not split on any variable in  $P$  due to the additive nature of Equation 2 and linearity of expectations. Furthermore, we may take advantage of the ensemble function's formulation in Equation 4 to remove any node whose path to root node does not split on any variable in  $P$ . This statement is made precise in Theorem 4.

**Theorem 4.** *Let  $\mathcal{E}(\cdot) = \sum_{k \in B_{\mathcal{E}}} \mu_k \mathbf{1}_{\mathbf{R}_k}(\cdot)$  be a BART ensemble. For any terminal node  $\eta_k$ , let  $v(k)$  be the index set of all split variables along the path to  $\eta_k$ 's root node. For any variable index set  $P$ , let*

$$\mathcal{E}_P(\cdot) := \sum_{\substack{k \in B_{\mathcal{E}} \\ v(k) \cap P \neq \emptyset}} \mu_k \mathbf{1}_{\mathbf{R}_k}(\cdot)$$

*be the ensemble function that results from removing from  $B_{\mathcal{E}}$  any terminal node whose path to root node does not split on any variable in  $P$ . Then*

$$\text{Var}_{\mathbf{X}_P}(\mathbb{E}[\mathcal{E}(\mathbf{X}) \mid \mathbf{X}_P]) = \text{Var}_{\mathbf{X}_P}(\mathbb{E}[\mathcal{E}_P(\mathbf{X}) \mid \mathbf{X}_P]).$$

To get a sense of how much computation Theorem 4 saves, consider the goal of computing all  $p$  (unnormalized) main-effects Sobol' indices for an arbitrary BART ensemble  $\mathcal{E}$ . To calculate  $V_i = \text{Var}_{X_i}(\mathbb{E}[\mathcal{E}(\mathbf{X}) \mid X_i])$

$X_i]$ ) for any variable  $x_i$  without Theorem 4, Equation 12 tells us that  $|B_{\mathcal{E}}|^2$  terms must be computed. Hence, computing all main-effects Sobol' indices would require  $p|B_{\mathcal{E}}|^2$  terms to be computed. But suppose we use Theorem 4 on a scenario where  $p \geq 5$  and  $N_1 = N_2 = N_3 = N_4 = N_5 = \frac{1}{4}|B_{\mathcal{E}}|$ , where  $N_i$  is the number of terminal nodes  $\eta_k$  in  $\mathcal{E}$  whose path to  $\eta_k$ 's root node includes split variable  $x_i$ . In this scenario, we impose the condition that if  $p > 5$ , then  $N_i = 0$  for all  $i > 5$ . Note that because  $\sum_{i=1}^p N_i > |B_{\mathcal{E}}|$ , the path of at least one terminal node contains more than one split variable. To calculate  $V_i$  for any variable  $x_i$ , Theorem 4 tells us that  $(\frac{1}{4}|B_{\mathcal{E}}|)^2$  terms must be computed for  $i = 1, 2, 3, 4, 5$  and zero terms must be computed for  $i > 5$ . Hence, computing all main-effects Sobol' indices would require  $\frac{5}{16}|B_{\mathcal{E}}|^2$  terms to be computed, which is at worst a 16-fold improvement over the case where Theorem 4 is not used. We stress that by using Theorem 4, the number of terms to compute is a function of  $|B_{\mathcal{E}}|^2$  and not also explicitly of  $p$ .

## 4.2 Total-effects index

In sensitivity analysis, we also often wish to obtain some measure of interaction between the input variables. We can do so via the total-effects sensitivity index, which is defined to be the sum of all normalized sensitivity indices involving the input variable in question (Saltelli et al., 2000). For example, if  $p = 3$ , then the total-effects index for input variable  $x_2$  would be  $T_2 = S_2 + S_{12} + S_{23} + S_{123}$ . Hence,  $T_2 - S_2$  provides a sense of the magnitude of all interactions involving variable  $x_2$ . However, in order to compute all  $p$  total-effects sensitivity indices, this formulation requires computing all  $2^p - 1$  normalized sensitivity indices  $S_P$ . Fortunately, the total-effects index turns out to be equivalent to the following more tractable definition: if  $f$  is a square-integrable function, then the total-effects index of  $f(\mathbf{X})$  for variable  $X_i$  is

$$T_i = 1 - \frac{\text{Var}_{\mathbf{X}_{-i}}(\mathbb{E}_{X_i}[f(\mathbf{X}) \mid \mathbf{X}_{-i}])}{\text{Var}(f(\mathbf{X}))}. \quad (14)$$

Note that  $\sum_{i=1}^p T_i \geq 1$  with equality only if the model is purely additive. Also note that the core of Equation 14, when applied to a BART ensemble function  $\mathcal{E}(\cdot)$ , is also the same variance expression  $\text{Var}_{\mathbf{X}_P}(\mathbb{E}[\mathcal{E}(\mathbf{X}) \mid \mathbf{X}_P])$  where  $P = \{1, \dots, i-1, i+1, \dots, p\}$ . Hence, we only need to compute  $p$  of these variance expressions in order to compute all  $p$  total-effects sensitivity indices.

# 5 Applications

## 5.1 Simulation study

**Simulation settings discussion.** Given data generated from Equation 1 and the true Sobol' index values for the mean  $f(\mathbf{x})$ , this section identifies the number of inputs, the sample size, and the magnitude of the measurement error standard deviation which answer the following questions:

- Q.1** What is the bias of BART-based Sobol' indices for estimating the true Sobol' indices when  $f(\mathbf{x})$  is measured with error?
- Q.2** How close are the main-effects rankings provided by BART-based Sobol' indices to the main-effects ranking provided by the true Sobol' indices?

**Q.3** How close are the main-effects rankings provided by one-way BART counts to the main-effects ranking provided by the true Sobol' indices?

For each simulation setting below, we generate a maximin LHS on  $[0, 1]^p$  with  $N$  runs (Carnell, 2019). Given a data-generating function  $f(\cdot): [0, 1]^p \rightarrow \mathbb{R}$ , we generate response values at each input point  $\mathbf{x}$  from Equation 1 where  $\epsilon \sim N(0, \sigma^2)$ . We generate 500 data sets for each possible combination of the following different parameter settings:  $p/p_0 \in \{1, 2, 3\}$ ,  $N \in \{10p, 50p\}$ , and  $\sigma^2 \in \{0.1\text{Var}(f(\mathbf{X})), 0.25\text{Var}(f(\mathbf{X}))\}$ , where  $p_0$  is the number of active (i.e. not inert) variables in  $f(\cdot)$  and  $\mathbf{X} = (X_1, \dots, X_p)$ , where each  $X_i \stackrel{iid}{\sim} U(0, 1)$ . For each  $f(\cdot)$ , the variance  $\text{Var}(f(\mathbf{X}))$  is calculated analytically where possible, otherwise numerical integral approximations are used. To each of these 500 data sets, we fit a BART model using the default parameter settings of the R BART package (McCulloch et al., 2019).

The three data-generation functions to be examined are:

1. From Friedman (1991), the data-generating function is defined as

$$f(\mathbf{x}) = 10 \sin(\pi x_1 x_2) + 20(x_3 - 0.5)^2 + 10x_4 + 5x_5.$$

This function, used in Chipman et al. (2010) and many other BART papers for variable activity and selection, is a challenging mix of interactions and nonlinearities. Here, only  $p_0 = 5$  variables influence the response. Also,  $\text{Var}(f(\mathbf{X})) \approx 23.8$ .

2. We modify the Friedman function above to create the data-generating function defined as

$$f(\mathbf{x}) = 10 \sin(\pi(x_1 - 0.5)(x_2 - 0.5)) + 20(x_3 - 0.5)^2 + 10x_4 + 5x_5.$$

In the original Friedman function, the main-effects Sobol' indices and the total-effects Sobol' indices have the same order. That is,  $S_1^f = S_2^f > S_4^f > S_3^f > S_5^f$  and  $T_1^f = T_2^f > T_4^f > T_3^f > T_5^f$  when  $f$  is the original Friedman function. For this modified version, however, the main-effects Sobol' indices for variables 1 and 2 are zero, which changes the order of the main-effects Sobol' indices while maintaining the total-effects order. Also,  $\text{Var}(f(\mathbf{X})) \approx 19.0$ .

3. The  $g$ -function from Saltelli and Sobol' (1995) with  $p_0$  inputs is defined to be

$$f(x_1, \dots, x_{p_0}) = \prod_{k=1}^{p_0} \frac{|4x_k - 2| + c_k}{1 + c_k},$$

where  $\mathbf{c} = (c_1, \dots, c_{p_0})$  has nonnegative components. This function is a product of univariate functions, which presents a more challenging environment to BART than do sums of univariate or bivariate functions. Here we use the coefficient values  $c_k = (k - 2)/2$  for  $k = 1, \dots, p_0$  suggested by Crestaux et al. (2009). We also use  $p_0 = 5$  active variables which gives us  $\text{Var}(f(\mathbf{X})) \approx 3.076$ .

Hence, we consider  $3 \times 2 \times 2 \times 3 = 36$  possible combinations of parameter settings and data-generating functions. We will call these the 36 simulation scenarios.

## 5.2 Performance metrics

We evaluate our results in terms of two metrics: the  $L_1$  performance metric and a rank-based performance metric.

Variable index $i$	Friedman			Modified Friedman			$g$ -function		
	$S_i^f$	$T_i^f$	$T_i^f - S_i^f$	$S_i^f$	$T_i^f$	$T_i^f - S_i^f$	$S_i^f$	$T_i^f$	$T_i^f - S_i^f$
1	0.197	0.274	0.077	0	0.335	0.335	0.433	0.701	0.268
2	0.197	0.274	0.077	0	0.335	0.335	0.108	0.284	0.176
3	0.093	0.093	0	0.117	0.117	0	0.048	0.135	0.087
4	0.350	0.350	0	0.438	0.438	0	0.027	0.078	0.051
5	0.087	0.087	0	0.110	0.110	0	0.017	0.050	0.033

Table 1:  $S_i^f$ ,  $T_i^f$ , and  $T_i^f - S_i^f$  for various data-generating functions  $f$ .

### $L_1$ performance metric

To answer question **Q.1** posed at the beginning of the section, we will first estimate the expectation of the  $L_1$  distance  $d_{L_1}(\cdot, \cdot)$  between BART-based Sobol' indices and the true Sobol' indices with respect to the BART posterior  $\pi(\Theta \mid \mathcal{D})$  from Equation 5. For example, if we are assessing the bias of BART-based main-effects Sobol' indices for a given number of inputs, sample size, and magnitude of the measurement error standard deviation (i.e for a given  $(p, N, \sigma^2)$ ), we will estimate the expectation

$$\int d_{L_1}(\mathbf{S}^{\mathcal{E}}, \mathbf{S}^f) d\pi(\Theta \mid \mathcal{D}) \approx \frac{1}{1000} \sum_{i=1}^{1000} d_{L_1}(\mathbf{S}^{\mathcal{E}^{(i)}}, \mathbf{S}^f) \quad (15)$$

using 1,000 posterior samples  $\{(\Theta^{(i)} \mid \mathcal{D})\}_{i=1}^{1000}$ , where the vectors  $\mathbf{S}^{\mathcal{E}} = (S_1^{\mathcal{E}}, S_2^{\mathcal{E}}, \dots, S_p^{\mathcal{E}})$  and  $\mathbf{S}^f = (S_1^f, S_2^f, \dots, S_p^f)$  contain the main-effects Sobol' indices of, respectively, BART ensemble function  $\mathcal{E}(\cdot)$  and data-generating function  $f(\cdot)$ . Here,  $\mathcal{E}(\cdot)$  is the BART ensemble function that results from posterior sample  $(\Theta \mid \mathcal{D})$  while each  $\mathcal{E}^{(i)}(\cdot)$  is similarly the BART ensemble function that results from the  $i$ th posterior sample  $(\Theta^{(i)} \mid \mathcal{D})$ . We will make similar estimates for two-way and total-effects Sobol' index calculations. Finally, we will estimate the expectation of the expected  $L_1$  distance with respect to generated data sets  $\mathcal{D}$ . In the example above, we will generate 500 values of the expected  $L_1$  distance estimate. The sample mean and standard deviation of these 500 estimates are shown in Table 2.

### Rank-based performance metric

To answer the remaining questions **Q.2** and **Q.3**, we replace the  $L_1$  distance  $d_{L_1}(\cdot, \cdot)$  in Equation 15 with a discrepancy measure  $d_r(\cdot, \cdot)$ , to be defined below in Equation 16. This allows a more interpretable comparison between the performances of one-way BART counts and BART-based Sobol' indices. The sample mean and standard deviation of these 500 estimates are shown in Table 3.

As an example, we will rank the normalized main-effects Sobol' index values  $(S_1, S_2, S_3, S_4, S_5) = (.197, .197, .093, .350, .087)$  of the Friedman function shown in Table 1 as  $(2, 2, 4, 1, 5)$ , where the most active variable (i.e. variable 4) gets ranking number 1 and the least active variable (i.e. variable 5) gets ranking number 5. Variables 1 and 2 are equally active, so we will adopt the convention used in many sports competitions of assigning the minimum rank to the two variables and then leaving a gap in the ranking numbers so that the positions of all variables less active than variables 1 and 2 are unaffected.

Several options exist for comparing two rankings. Kendall (1948) introduces a distance that, when ties in rankings are not allowed, is the graphical distance between two vertices in the well-studied permutation

	$(p, N, \sigma^2)$	$S_i^f$ vs $S_i^\varepsilon$	$S_{ij}^f$ vs $S_{ij}^\varepsilon$	$T_i^f$ vs $T_i^\varepsilon$
Friedman function	(5, 50p, 0.10)	0.0734 (0.0248)	0.0718 (0.0107)	0.139 (0.0449)
	(5, 50p, 0.25)	0.0992 (0.0367)	0.0824 (0.00643)	0.165 (0.0482)
	(5, 10p, 0.10)	0.183 (0.0652)	0.0883 (0.00198)	0.256 (0.0905)
	(5, 10p, 0.25)	0.222 (0.0829)	0.0904 (0.00228)	0.287 (0.0987)
	(10, 50p, 0.10)	0.0785 (0.0191)	0.0812 (0.0236)	0.192 (0.0512)
	(10, 50p, 0.25)	0.12 (0.0283)	0.0878 (0.0112)	0.236 (0.0387)
	(10, 10p, 0.10)	0.214 (0.0519)	0.0993 (0.00349)	0.348 (0.0583)
	(10, 10p, 0.25)	0.287 (0.0623)	0.103 (0.00385)	0.424 (0.07)
	(15, 50p, 0.10)	0.0813 (0.0233)	0.0916 (0.0353)	0.216 (0.0723)
	(15, 50p, 0.25)	0.119 (0.0227)	0.0912 (0.0204)	0.256 (0.0459)
	(15, 10p, 0.10)	0.224 (0.0438)	0.102 (0.00431)	0.376 (0.0495)
	(15, 10p, 0.25)	0.321 (0.0551)	0.108 (0.00458)	0.482 (0.0625)
Modified Friedman function	(5, 50p, 0.10)	0.101 (0.0256)	0.0403 (0.0178)	0.14 (0.0641)
	(5, 50p, 0.25)	0.114 (0.0328)	0.0721 (0.0295)	0.125 (0.0552)
	(5, 10p, 0.10)	0.33 (0.0412)	0.337 (0.0101)	0.724 (0.0673)
	(5, 10p, 0.25)	0.345 (0.0518)	0.346 (0.00578)	0.696 (0.0753)
	(10, 50p, 0.10)	0.151 (0.0253)	0.0736 (0.0267)	0.278 (0.0793)
	(10, 50p, 0.25)	0.167 (0.0273)	0.0537 (0.0182)	0.204 (0.0525)
	(10, 10p, 0.10)	0.276 (0.0575)	0.268 (0.0383)	0.668 (0.114)
	(10, 10p, 0.25)	0.361 (0.0615)	0.336 (0.0239)	0.842 (0.0841)
	(15, 50p, 0.10)	0.169 (0.0248)	0.0967 (0.0272)	0.349 (0.0794)
	(15, 50p, 0.25)	0.185 (0.0246)	0.0534 (0.0187)	0.257 (0.0662)
	(15, 10p, 0.10)	0.229 (0.0428)	0.191 (0.0345)	0.509 (0.0886)
	(15, 10p, 0.25)	0.345 (0.059)	0.285 (0.0376)	0.779 (0.104)
g-function	(5, 50p, 0.10)	0.334 (0.0408)	0.258 (0.0138)	0.385 (0.0597)
	(5, 50p, 0.25)	0.365 (0.0552)	0.265 (0.00853)	0.44 (0.0692)
	(5, 10p, 0.10)	0.499 (0.112)	0.282 (0.00282)	0.587 (0.113)
	(5, 10p, 0.25)	0.55 (0.12)	0.28 (0.00296)	0.651 (0.123)
	(10, 50p, 0.10)	0.314 (0.0471)	0.251 (0.0384)	0.428 (0.0617)
	(10, 50p, 0.25)	0.36 (0.0563)	0.315 (0.0168)	0.553 (0.0571)
	(10, 10p, 0.10)	0.505 (0.0972)	0.329 (0.00453)	0.772 (0.091)
	(10, 10p, 0.25)	0.589 (0.104)	0.331 (0.00439)	0.872 (0.1)
	(15, 50p, 0.10)	0.299 (0.0381)	0.198 (0.0422)	0.384 (0.0597)
	(15, 50p, 0.25)	0.349 (0.0496)	0.297 (0.0341)	0.544 (0.0646)
	(15, 10p, 0.10)	0.497 (0.0935)	0.344 (0.00665)	0.832 (0.0843)
	(15, 10p, 0.25)	0.57 (0.105)	0.348 (0.00647)	0.949 (0.0982)

Table 2: Estimates of the expected  $L_1$  distance between BART-based Sobol' indices and true Sobol' indices when  $f(\mathbf{x})$  is measured with error. Here,  $S_i$  refers to the normalized main-effects Sobol' index of variable  $i$ ,  $S_{ij}$  refers to the normalized two-way Sobol' index of variables  $i$  and  $j$ , and  $T_i$  refers to the normalized total-effects Sobol' index of variable  $i$ . Each set of four scenarios (i.e. each set of four rows) is ordered roughly in decreasing order of "signal-to-noise."

	$(p, N, \sigma^2)$	$S_i^{\mathcal{E}}$ vs $S_i^f$	Cnt vs $S_i^f$	$T_i^{\mathcal{E}}$ vs $T_i^f$	Cnt vs $T_i^f$	$S_{ij}^{\mathcal{E}}$ vs $S_{ij}^f$
Friedman function	Max value	20	20	20	20	20
	(5, 50p, 0.10)	0.952 (1)	5.54 (1.48)	0.956 (1)	5.54 (1.48)	0.664 (3.28)
	(5, 50p, 0.25)	1.11 (1)	5.75 (1.98)	1.1 (0.996)	5.75 (1.98)	0.028 (0.346)
	(5, 10p, 0.10)	2.18 (1.66)	5.43 (3.39)	2.17 (1.65)	5.43 (3.39)	2.22 (2.8)
	(5, 10p, 0.25)	2.64 (1.92)	5.88 (3.42)	2.64 (1.91)	5.88 (3.42)	4.39 (4.3)
	Max value	70	70	70	70	90
	(10, 50p, 0.10)	0.912 (0.997)	5.89 (1.97)	0.876 (0.993)	5.89 (1.97)	19 (36)
	(10, 50p, 0.25)	0.988 (1)	6.6 (2.46)	0.98 (1)	6.6 (2.46)	4.62 (19.4)
	(10, 10p, 0.10)	1.52 (1.18)	5.69 (3.63)	1.51 (1.16)	5.69 (3.63)	0.912 (1.93)
	(10, 10p, 0.25)	2.07 (1.46)	6.85 (4.31)	2.03 (1.43)	6.85 (4.31)	3.49 (6.56)
	Max value	120	120	120	120	210
	(15, 50p, 0.10)	0.74 (0.967)	4.92 (1.36)	0.772 (1.06)	4.92 (1.36)	86.2 (102)
	(15, 50p, 0.25)	1 (1)	5.74 (2.29)	0.98 (1)	5.74 (2.29)	39.1 (81)
	(15, 10p, 0.10)	1.52 (0.907)	3.88 (3.11)	1.52 (0.912)	3.88 (3.11)	0.412 (1.56)
	(15, 10p, 0.25)	1.69 (1.3)	5.34 (4.48)	1.68 (1.3)	5.34 (4.48)	1.9 (4.41)
Modified Friedman function	Max value	20	20	20	20	20
	(5, 50p, 0.10)	0.948 (1)	13.4 (1.42)	2.1 (2.06)	5.42 (1.42)	0 (0)
	(5, 50p, 0.25)	1.06 (0.999)	13.6 (1.47)	1.24 (1.27)	5.55 (1.47)	0 (0)
	(5, 10p, 0.10)	1.7 (0.985)	7.3 (3.71)	9.26 (1.16)	5.56 (3.35)	0 (0)
	(5, 10p, 0.25)	1.96 (1.35)	6.55 (3.72)	9.06 (1.39)	6.39 (3.41)	0 (0)
	Max value	70	70	70	70	90
	(10, 50p, 0.10)	0.792 (0.979)	13.7 (1.92)	3.91 (1.89)	5.67 (1.92)	0 (0)
	(10, 50p, 0.25)	0.976 (1)	14.4 (2.37)	1.84 (1.96)	6.39 (2.37)	0 (0)
	(10, 10p, 0.10)	1.6 (0.847)	12.2 (3.41)	5.19 (3.27)	5.18 (3.06)	0 (0)
	(10, 10p, 0.25)	1.78 (1.5)	9.84 (5.01)	9.27 (3.28)	7.39 (5.04)	0 (0)
	Max value	120	120	120	120	210
	(15, 50p, 0.10)	0.768 (0.974)	12.8 (1.17)	4.52 (1.31)	4.84 (1.17)	0 (0)
	(15, 50p, 0.25)	0.968 (1)	13.5 (1.87)	2.88 (2.15)	5.45 (1.87)	0 (0)
	(15, 10p, 0.10)	1.43 (0.903)	12.4 (2.75)	1.66 (1.4)	4.58 (2.68)	0 (0)
	(15, 10p, 0.25)	1.48 (0.938)	10.9 (4.49)	4.72 (3.37)	5.23 (4.15)	0 (0)
g-function	Max value	20	20	20	20	90
	(5, 50p, 0.10)	0.676 (1.06)	2.36 (1.98)	0.716 (1.06)	2.36 (1.98)	23.7 (8.49)
	(5, 50p, 0.25)	1.11 (1.3)	3.22 (2.44)	1.09 (1.29)	3.22 (2.44)	29.3 (9.71)
	(5, 10p, 0.10)	2.99 (2.43)	4.41 (3.08)	3.02 (2.41)	4.41 (3.08)	38.4 (10.6)
	(5, 10p, 0.25)	3.88 (2.65)	5.55 (3.42)	3.88 (2.65)	5.55 (3.42)	38.9 (11.1)
	Max value	70	70	70	70	790
	(10, 50p, 0.10)	0.336 (0.78)	1.59 (1.8)	0.404 (0.823)	1.59 (1.8)	93.3 (39.2)
	(10, 50p, 0.25)	0.752 (1.12)	3.26 (2.9)	0.764 (1.16)	3.26 (2.9)	155 (48.5)
	(10, 10p, 0.10)	3.35 (2.86)	7.77 (5.05)	3.35 (2.88)	7.77 (5.05)	254 (63.4)
	(10, 10p, 0.25)	4.77 (3.57)	9.85 (5.87)	4.72 (3.59)	9.85 (5.87)	265 (65)
	Max value	120	120	120	120	1990
	(15, 50p, 0.10)	0.224 (0.644)	0.88 (1.28)	0.364 (0.783)	0.88 (1.28)	149 (82.4)
	(15, 50p, 0.25)	0.432 (0.834)	1.6 (1.98)	0.444 (0.851)	1.6 (1.98)	244 (97.5)
	(15, 10p, 0.10)	2.26 (2.31)	5.38 (4.8)	2.24 (2.27)	5.38 (4.8)	486 (142)
	(15, 10p, 0.25)	4.45 (4.43)	9.07 (6.58)	4.42 (4.35)	9.07 (6.58)	531 (146)

Table 3: Estimates of the expected  $d_r$  discrepancy between BART-based Sobol’ index rankings and true Sobol’ index rankings when  $f(\mathbf{x})$  is measured with error. Here,  $S_i$  refers to the normalized main-effects Sobol’ index of variable  $i$ ,  $S_{ij}$  refers to the normalized two-way Sobol’ index of variables  $i$  and  $j$ , and  $T_i$  refers to the normalized total-effects Sobol’ index of variable  $i$ . Each set of four scenarios (i.e. each set of four rows) is ordered roughly in decreasing order of “signal-to-noise.”

polytope that represents all possible rankings of  $p$  objects (Heiser and D’Ambrosio, 2013). Emond and Mason (2002) point out that when ties are allowed, Kendall’s “distance” violates the triangle inequality and hence is no longer a true metric. They advocate the distance defined by Kemeny and Snell (1962), which equals Kendall’s distance when ties are not allowed, but remains a metric when ties are allowed.

Unfortunately, the Kemeny-Snell (KS) distance is likely to artificially inflate when the data-generating function has either more than two inert variables or has equally-active non-inert variables. In the former scenario, a fitted BART model is unlikely to entirely shrink all of its input activity measures of the inert variables. In this case, the KS distance will be inflated by the fitted BART model assigning small but positive effects to the inert variables. In the latter scenario, a fitted BART model is unlikely to perfectly match its input activity measures of the equally-active non-inert variables. In this case, the fitted BART model could be incorrectly “punished” for even the slightest discrepancy between the variable-activity measures of two equally-active variables. To resolve this issue, we create a discrepancy measure based on the multi-stage discordance measures discussed in Fligner and Verducci (1988).

To compute the discordance measures between two rankings  $\rho_f$  and  $\rho_\varepsilon$ , where in our variable activity setting  $\rho_f$  represents the true input activity and  $\rho_\varepsilon$  represents the input activity of our fitted BART model, Fligner and Verducci (1988) assume that neither ranking has any ties. As an example, suppose  $\rho_f = (4, 3, 1, 2)$  and  $\rho_\varepsilon = (3, 1, 2, 4)$ . The discordances  $W_1, W_2, \dots, W_4$  will be computed sequentially. To compute discordance  $W_1$ , we see that variable 3 is the most active in  $\rho_f$ . Since variable 3 is the second most active in  $\rho_\varepsilon$ , we set  $W_1 = 2 - 1 = 1$ . We then remove variable 3 from consideration to compute  $W_2, W_3$ , and  $W_4$ . To compute discordance  $W_2$ , we see that variable 4 is the most active of the remaining variables (1, 2, and 4) in  $\rho_f$ . Since variable 4 is the third most active of the remaining variables (1, 2, and 4) in  $\rho_\varepsilon$ , we set  $W_2 = 3 - 1 = 2$ . We then remove variable 4 from consideration to compute discordances  $W_3$  and  $W_4$ . To compute  $W_3$ , we see that variable 2 is the most active of the remaining variables (1 and 2) in  $\rho_f$ . Since variable 2 is the most active of the remaining variables (1 and 2) in  $\rho_\varepsilon$ , we set  $W_3 = 1 - 1 = 0$ . We then remove variable 2 from consideration to compute  $W_4$ . Since only one variable remains, we set  $W_4 = 0$ . Hence, the discordances in this example are  $(W_1, W_2, W_3, W_4) = (1, 2, 0, 0)$ .

More generally (but still assuming neither ranking has any ties), suppose we have already computed discordances  $W_1, \dots, W_{k-1}$  for some  $k = 1, \dots, q$ , where  $q$  is the number of elements in vector  $\rho_f$ , and wish to compute  $W_k$ . Note that  $q$  is not necessarily  $p$  (e.g.  $q = \binom{p}{2}$  when the rankings represent two-way interactions). Thus, we have removed  $k - 1$  of the  $q$  items (e.g. variables, variable pairs, variable tripets) from consideration. If item  $i$  is the most active in ranking  $\rho_f$  among the remaining considered items, we then find  $j$ , where item  $i$  is the  $j$ th most active in ranking  $\rho_\varepsilon$  among the remaining considered items. The value  $W_k$  is then set to be  $j - 1$ .

Now suppose both ranking  $\rho_f$  and ranking  $\rho_\varepsilon$  are allowed to have ties. As mentioned earlier, we will adopt the “standard competition” ranking convention of, for each set of items tied with each other, assigning the minimum rank to the tied items and then leaving a gap in the ranking numbers so that the positions of all items less active than the tied items are unaffected. For example, main-effects Sobol’ index values (0.1, 0.1, 0.2, 0.2, 0.35, 0.05) would be ranked (4, 4, 2, 2, 1, 6). Suppose we have already computed  $W_1, \dots, W_{k-1}$  for some  $k = 1, \dots, q$  and wish to compute  $W_k$ . If  $u \geq 1$  items  $i_1, \dots, i_u$  are tied for most active in ranking  $\rho_f$  among the remaining considered items, we can find  $j_1, \dots, j_u$ , where item  $i_l$  is the  $j_l$ th most active item in ranking  $\rho_\varepsilon$  among the remaining considered items. The value  $W_k$  is then set to be  $\min_{l=1, \dots, u} j_l - 1$ . If  $\text{argmin}_{l=1, \dots, u} j_l$  has more than one value, then we pick any one (it does not matter which) of the corresponding items  $i_l$  to remove from consideration. Once an item is removed from consideration, the value  $W_{k+1}$  can then be computed (if  $k < p$ ). Note that if  $u = 1$ , this reduces to the “no-ties” case.



We can now define our discrepancy measure between rankings  $\rho_f$  and  $\rho_{\mathcal{E}}$ :

$$d_r(\rho_f, \rho_{\mathcal{E}}) = 2 \sum_{k=1}^q W_k, \quad (16)$$

where discordances  $W_1, W_2, \dots, W_q$  are computed as described in the previous paragraph. This measure has three particularly desirable properties. First, it equals Kendall's distance (and hence the KS distance) when ties are not allowed. Second, it does not inflate as the number of data-generating function  $f(\cdot)$ 's inert variables increases. In particular, discordance  $W_k = 0$  for all  $k > q_0$ , where  $q_0$  is the number of active items (i.e. items with non-zero input activity measure) in  $f$ . Hence, the discrepancy measure is invariant to the number of inert variables. Third, it does not inflate when  $f(\cdot)$  has equally-active non-inert items. If  $f$  has a set of equally-active non-inert items, then the discrepancy measure will not inflate as long as the equally-active items in the set are consecutively ranked. These three properties can be stated as Theorems 5, 6, and 7 whose proofs are in the appendix.

**Theorem 5.** *If rankings  $\alpha$  and  $\beta$  each have no ties, then the Kemeny-Snell distance between  $\alpha$  and  $\beta$  equals the discrepancy measure  $d_r(\alpha, \beta)$  in Equation 16.*

**Theorem 6.** *Consider the discrepancy  $d_r(\rho_f, \rho_{\mathcal{E}})$  between rankings  $\rho_f$  and  $\rho_{\mathcal{E}}$ . Then discordance  $W_k = 0$  for all  $k > q_0$ , where  $q_0$  is the number of active items in  $f$ .*

**Theorem 7.** *Consider the discrepancy  $d_r(\rho_f, \rho_{\mathcal{E}})$  between rankings  $\rho_f$  and  $\rho_{\mathcal{E}}$ . Suppose  $u \geq 1$  items  $i_j, \dots, i_{j+u-1}$  (and no other items) have ranking number  $j$  in  $\rho_f$  and ranking numbers  $r_j, \dots, r_{j+u-1}$  in  $\rho_{\mathcal{E}}$ . Then all  $|\rho_f|$  discordances are invariant to choice of permutation  $\phi$  of set  $\{r_j, \dots, r_{j+u-1}\}$  of ranking numbers.*

### 5.3 Simulation results

To answer question **Q.1**, we make several observations in Table 2. Unsurprisingly, the  $L_1$  distances for all three data-generating functions and all three Sobol' index measures tend to increase with each of increasing noise, decreasing sample size, and increasing amount of inert variables. That is, the BART-based Sobol' indices perform better as "signal-to-noise" ratio increases.

Interestingly, for each set of four scenarios, the performance difference between data scenarios ( $N = 50p, \sigma^2 = 0.10\text{Var}(f(\mathbf{X}))$ ) and ( $N = 50p, \sigma^2 = 0.25\text{Var}(f(\mathbf{X}))$ ) is much smaller than the performance differences between  $(50p, 0.25)$  and  $(10p, 0.10)$  and between  $(10p, 0.10)$  and  $(10p, 0.25)$ . We might infer that the  $N = 50p$  scenario saturates the data with enough signal for modest noise increases to not make much of a performance difference, but the change from  $50p$  to  $10p$  makes the signal so scarce that modest noise increases does make a performance difference.

We also note in the  $(p = 5, N = 50p, \sigma^2 = 0.10\text{Var}(f(\mathbf{X})))$  and  $(p = 5, N = 50p, \sigma^2 = 0.25\text{Var}(f(\mathbf{X})))$  scenarios, BART captures both the main-effects and total-effects indices of the modified Friedman function quite well. This is of particular interest because the discrepancy between the main-effects and total-effects indices of the modified Friedman function for variables 1 and 2 is so large (see Table 1). BART's performance on the modified Friedman function implies that with enough signal, it is able to distinguish the zero marginal effects and the large total effects of variables 1 and 2. That is, BART seems to tell if an input is important on its own or if it interacts strongly with other inputs.

Also perhaps unsurprisingly, BART performs worse with the multiplicative  $g$ -function than it does with the two additive data-generating functions. Both the Friedman function and modified Friedman function are sums of either univariate or bivariate functions which BART’s additive structure can presumably capture well. On the other hand, our  $g$ -function is a product of five univariate functions. If we note that the log of our  $g$ -function is also a sum of univariate functions, we might expect BART to perform better if we took the log of the  $g$ -function response data.

Finally, BART tends to capture total-effects indices less accurately than it does main-effects indices. Interestingly, this observation holds even for the high-signal scenarios.

To answer questions **Q.2** and **Q.3**, we make several striking observations in Table 3. First, our BART-based main-effects Sobol’ indices perform incredibly well at predicting the correct order of the true main-effects Sobol’ indices across all data scenarios for both the original Friedman function and modified Friedman function and across the  $N = 50p$  scenarios for the  $g$ -function.

Second, our BART-based Sobol’ indices outperform one-way BART counts across the board when predicting the correct order of the true main-effects Sobol’ indices and of the true total-effects Sobol’ indices. Hence, our BART-based main-effects and total-effects Sobol’ indices should always be preferred over one-way counts.

Finally, the one-way BART counts match the true total-effects Sobol’ indices more closely than the true main-effects Sobol’ indices in the modified Friedman function (the order of the true main-effects Sobol’ indices and the true total-effects Sobol’ indices are the same for both the original Friedman function and the  $g$ -function). In this particular example, the one-way BART counts seem to be a better reflection of the true total-effects Sobol’ indices than of the true main-effects Sobol’ indices.

We conclude that our BART-based main-effects Sobol’ indices can accurately predict the raw values of main-effects Sobol’ indices of additive data-generating functions. Also, our BART-based main-effects and total-effects Sobol’ indices can accurately predict the rankings of, respectively, main-effects Sobol’ indices and total-effects Sobol’ indices of both additive and multiplicative data-generating functions. Finally, our BART-based main-effects and total-effects Sobol’ indices outperform one-way BART counts for all three data-generating functions.

## 5.4 Application to En-ROADS Climate Simulator

We compute Sobol’ indices for a BART model trained on data generated from the En-ROADS climate simulator (Climate Interactive et al., 2020). This simulator is a mathematical model of how global temperature and carbon emissions, among other factors, are influenced by changes in energy, land use, consumption, agriculture, and other policies. It is designed to be easily used by policymakers, educators, and the general public. The model, an ordinary differential equation solved by Euler integration, synthesizes what its developers consider to be the best available climate science. This simulator is available from the Climate Interactive website.

For this paper, we looked specifically at how the average global temperature increase by 2100 from pre-industrial levels is influenced by the 18 “top-level” input variables shown when the En-ROADS climate simulator is first loaded on to a web browser. We explored a subset of 11 variables as summarized in Fig 5 and left the remaining 7 variables at their default settings. Each input variable is bounded by a minimum and maximum value. We found a maximin LHS design of  $10 \times 11 = 110$  points on  $[0, 1]^{11}$  and scaled it so that the design space contained the range of possible values. However, the simulator rounds values entered into its text fields, effectively rounding each design point to the nearest point on the induced 11-dimensional grid. We then manually obtained response values for each design point. The simulator

also rounded the response values to the nearest first decimal place. Because a  $0.1^{\circ}F$  difference is smaller than a  $0.1^{\circ}C$  difference, we used Fahrenheit values. We then rescaled this “rounded” maximin LHS design back onto  $[0, 1]$ <sup>11</sup> to which we trained a BART model with the default parameter settings of, in particular, 10,000 posterior samples from the distribution in Equation 5 and 200 trees.

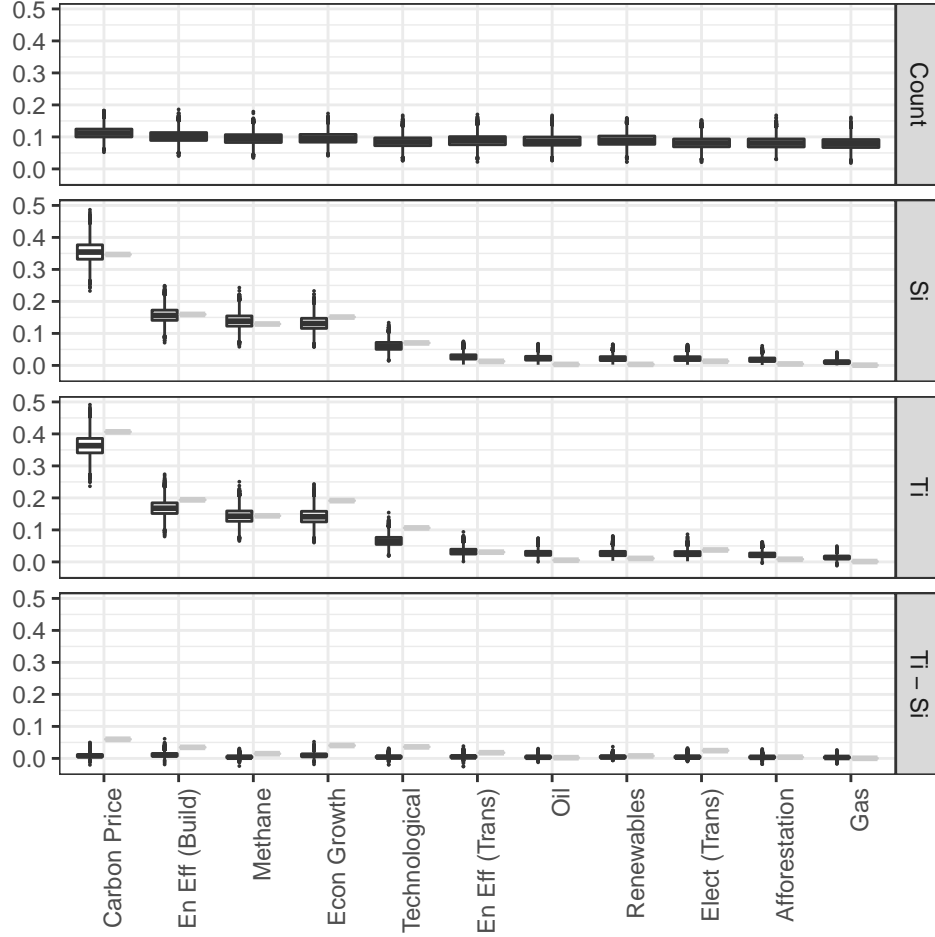


Figure 5: Variable activity measures of BART and GP models trained on data from En-ROADS climate simulator. Variable counts (top panel), BART-based main-effects Sobol’ indices (second panel), BART-based total-effects Sobol’ indices (third panel), and the difference between total-effects and main-effects (bottom panel) are shown. Variable activity measures of the 10,000 ensembles corresponding to posterior samples of the trained BART model are shown in black. Point estimates of Sobol’ indices of the trained GP model based on the same data are shown in grey.

We computed the main-effects, two-way, and total-effects Sobol’ indices of the BART model trained on our collected climate simulator data. Because main effects account for more than 96% of the BART model’s total variance, we do not show two-way Sobol’ indices. By taking the mean main-effects Sobol’ indices of the 11 input variables over the 10,000 posterior samples, we see in Figure 5 that carbon price accounts for 35.1% of the BART model’s total variance, which is twice as much as the next largest impacts of energy efficiency of buildings and industry at 16.1%, methane and other (which includes nitrous oxide and fluorinated gases) at 14.4%, and economic growth at 13.1%. The total-effects Sobol’ indices imply a

similar conclusion. Variable counts, however, fail to provide evidence of such large differences in impacts of the input variables.

For comparison, we also estimated sensitivity indices and created range plots by fitting a constant mean Gaussian process (GP) model (i.e. kriging model) to the training data (Han et al., 2009). In Figure 5, we see that the Sobol’ indices of the trained BART model match those of the trained kriging model quite well. We also see that the one-way counts of the trained BART model poorly matches both the main-effects and total-effects Sobol’ indices of the trained kriging model, which supports the hypothesis that the variable count heuristic is not a meaningful input activity measure. In Figure 6, we show range plots of the four most active input variables. For each input, we approximated the marginal response at each of 10 equally spaced points by varying the remaining inputs using a  $2^9$ -point Sobol’ sequence design (Kuo and Joe, 2017). In the left two plots (carbon price and energy efficiency of buildings and industry), the response and its slope decrease with increasing input values. In the right two plots (economic growth and methane & other), the response and its slope increase with increasing input values. Hence, all four of these input variables seem to marginally have diminishing effects on future temperature increase.

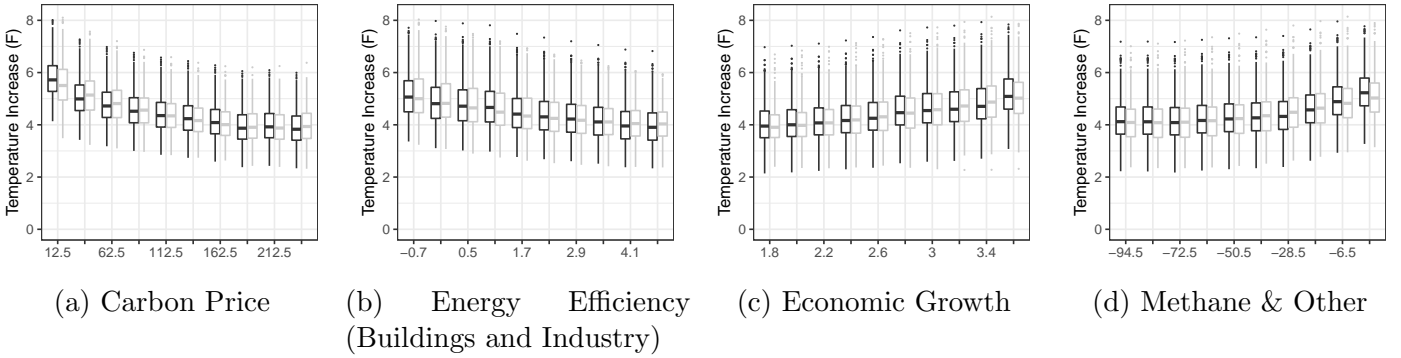
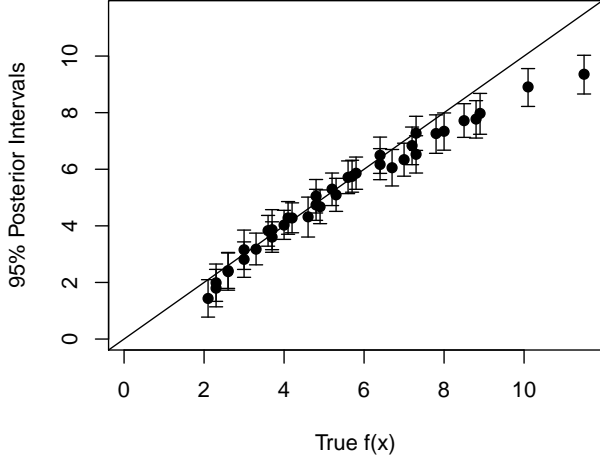


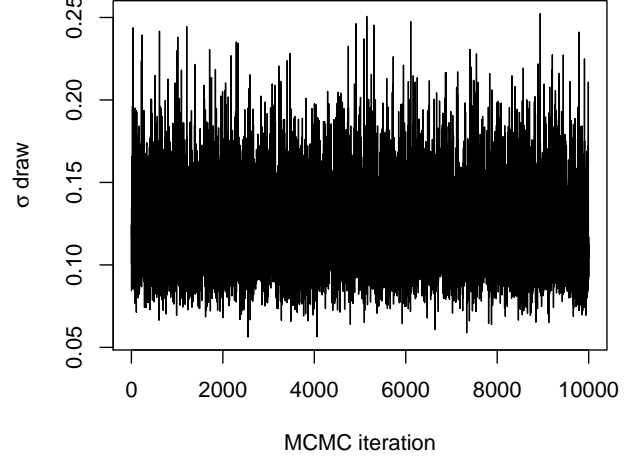
Figure 6: Range plots of the four most active input variables. The trained BART model is shown in black while the trained GP model is shown in grey.

To assess prediction accuracy, we predicted temperature increases from an out-of-sample test set of 37 samples, which are chosen manually to achieve a wide range of true temperature increase values. Figure 7a shows that the BART model accurately predicts temperature increase at, roughly, mid-range values of  $f(\mathbf{x}) \in [2.5^\circ F, 7.5^\circ F]$ . Outside of this range, the BART model tends to underpredict temperature increase. We suspect this underprediction issue at the upper range is due to the training points having a maximum global temperature increase value of  $7.8^\circ F$  and hence can be fixed by adding more training samples with extreme response values, which can be done by using combinations of extreme values of the four most active input variables. We also see in Figure 7b that the  $\sigma$  samples appear to be stationary, which implies MCMC convergence.

We conclude that in this no-noise application with  $p = 11$  predictors, a sample size of  $N = 10p$  suffices for a trained BART model to adequately capture input importance through its Sobol’ indices. Variable counts, on the other hand, do not provide enough evidence to convincingly order variables in terms of their importance.



(a) Posterior prediction intervals (PPIs) for 37 out-of-sample test values of  $f(\mathbf{x})$ . For each test input point  $\mathbf{x}$ , error bars reflect the 0.025 and 0.975 quantiles of the 10,000 posterior predictions of  $f(\mathbf{x})$ .



(b) Trace plot for posterior draws of  $\sigma$ .

Figure 7: Diagnostic plots of BART model trained on data from En-ROADS climate simulator.

## 6 Summary and Discussion

This paper has provided analytic expressions, explicit interpretations, and computational algorithms for determining Sobol' indices for BART models. The indices are computed exactly and avoid Monte Carlo approximations. We showed the relationship between Sobol' indices for BART models and sensitivity indices obtained from one-way counts, which are the predominant way of assessing input activity in BART (see Bleich et al. (2014); Linero (2018) among others). Theorem 2 showed that under certain conditions, both the one-way count and the main-effects Sobol' index of variable  $x_i$  are functions of the conditional expectation function  $\mathbb{E}_{\mathbf{X}_{-i}}[\mathcal{E}(\mathbf{X})|X_i = \cdot]$ . We then quantify the properties of Sobol' indices estimated from the BART model for three different analytic functions. First the bias and the uncertainty of the BART-based Sobol' indices for estimating the true Sobol' indices for the underlying  $f(\cdot)$  are estimated. Then the rankings of variable activity as measured by the BART-based Sobol' indices are compared with those provided by one-way counts. To make the second comparisons, we proposed a rank discrepancy  $d_r$  to better suit the problem of comparing input activity assessments.

Finally, we applied our BART-based Sobol' indices to data generated by the En-ROADS climate simulator to explore how to best reduce future global temperature increases. In particular we note that 32 of the 37 input values in Figure 7a and 109 of the 110 training inputs result in future global temperature increases above  $1.5^\circ\text{C}$  ( $2.7^\circ\text{F}$ ), which is the agreed upon upper limit of average global temperature increase above pre-industrial levels set by the 2016 Paris Agreement under the United Nations Framework Convention on Climate Change (UNFCCC, 2015). In words, the vast majority of policy scenarios described in Section 5 will result in global temperature increases of at least  $1.5^\circ\text{C}$  by the year 2100. Indeed, a 2018 report from the Intergovernmental Panel on Climate Change claims that this temperature increase will likely reach

1.5°C between 2030 and 2052 if it increases at its current rate (IPCC, 2018). The IPCC report also details the global impact of a 1.5°C increase. Given these drastic predictions it is imperative to identify the most impactful factors in minimizing this temperature increase. To achieve a temperature increase below 1.5°C by 2100, Figures 5 and 6 suggest maximizing carbon price and the energy efficiency of buildings and industry while minimizing economic growth and the use of methane and other gases (which includes nitrous oxide and fluorinated gases).

This research suggests additional statistical investigations. Linero (2018) shows empirically that when a Dirichlet prior is used to generate variable selection probabilities for tree nodes, the posterior probability of an arbitrary inert variable being included in a BART model can drastically shrink. If inert variables are simply not used in a BART model’s split rules, then Theorem 4 tells us that computing all Sobol’ indices up to some order will require fewer calculations. Furthermore, excluding inert variables might also improve the accuracy or efficiency of our BART-based Sobol’ indices. These observations suggest comparing the accuracy of our BART-based Sobol’ indices using a Dirichlet prior with those obtained from the default prior as well as the effect of increasing sample sizes.

As has been noted, Bleich et al. (2014) and Linero (2018), among others, use variable counts in their variable selection methods for BART models. We have seen in the En-ROADS climate simulator example that a trained BART model better captures input activity through its Sobol’ indices rather than through one-way counts. This example suggests that additional research is needed to study the specificity and sensitivity in selecting active inputs for the two methods in order definitively draw this conclusion.

We conclude with two important data/model extensions. Our derivation of the Sobol’ index calculations assumed that the input variables are uncorrelated. Of course, this is not true in many applications. For dependent input variables it will be very useful to derive analytic expressions for BART-based Sobol’ indices. Here ideas from Kucherenko et al. (2012), Mara and Tarantola (2012), and Glen and Isaacs (2012), who all discuss various ways to estimate Sobol’ sensitivity indices in the dependent input variable case will be of use. Finally, we note that most of the results in the paper should extend to other tree ensemble methods, such as the random forest method described in Breiman (2001).

## ACKNOWLEDGMENTS

A.H. would like to acknowledge the Graduate School at The Ohio State University for support during the dissertation year. The work of M.T.P. was supported in part by the National Science Foundation under Agreement DMS-1916231 and in part by the King Abdullah University of Science and Technology (KAUST) Office of Sponsored Research (OSR) under Award No. OSR-2018-CRG7-3800.3. T.J.S. would like to thank the Isaac Newton Institute for Mathematical Sciences for support and hospitality during the programme on *Uncertainty Quantification* when work on this paper was undertaken. This research was also sponsored, in part, by the National Science Foundation under Agreements DMS-0806134 and DMS-1310294 (The Ohio State University).

## References

- Bengtsson, H. (2019). *matrixStats: Functions that Apply to Rows and Columns of Matrices (and to Vectors)*. R package version 0.55.0.
- Bleich, J., A. Kapelner, E. I. George, and S. T. Jensen (2014, 09). Variable selection for bart: An application to gene regulation. *Ann. Appl. Stat.* 8(3), 1750–1781.

- Breiman, L. (2001). Random forests. *Machine Learning* 45, 5–32.
- Carnell, R. (2019). *lhs: Latin Hypercube Samples*. R package version 1.0.1.
- Chipman, H., P. Ranjan, and W. Wang (2012). Sequential design for computer experiments with a flexible bayesian additive model. *Canadian Journal of Statistics* 40(4), 663–678.
- Chipman, H. A., E. I. George, and R. E. McCulloch (1998). Bayesian cart model search. *Journal of the American Statistical Association* 93, 935–948.
- Chipman, H. A., E. I. George, and R. E. McCulloch (2010). Bart: Bayesian additive regression trees. *The Annals of Applied Statistics* 4, 266–298.
- Climate Interactive, Ventana Systems, Todd Fincannon, UML Climate Change Initiative, and MIT Sloan (2020). En-ROADS climate change solutions simulator. <https://en-roads.climateinteractive.org/scenario.html?v=2.7.15>. Accessed: 2020-04-03.
- Crestaux, T., O. L. Maître, and J.-M. Martinez (2009). Polynomial chaos expansion for sensitivity analysis. *Reliability Engineering & System Safety* 94(7), 1161 – 1172. Special Issue on Sensitivity Analysis.
- Emond, E. J. and D. W. Mason (2002). A new rank correlation coefficient with application to the consensus ranking problem. *Journal of Multi-Criteria Decision Analysis* 11(1), 17–28.
- Fligner, M. A. and J. S. Verducci (1988). Multistage ranking models. *Journal of the American Statistical association* 83(403), 892–901.
- Friedman, J. H. (1991). Multivariate adaptive regression splines. *The annals of statistics* 19(1), 1–67.
- Glen, G. and K. Isaacs (2012). Estimating sobol’ sensitivity indices using correlations. *Environmental Modelling & Software* 37, 157–166.
- Gramacy, R. B. and B. Haaland (2016). Speeding up neighborhood search in local gaussian process prediction. *Technometrics* 58(3), 294–303.
- Han, G., T. J. Santner, and H. Moon (2009). Matlab parametric empirical kriging (mperk) user’s guide. [https://www.asc.ohio-state.edu/statistics/comp\\_exp/jour.club/MperkManual.pdf](https://www.asc.ohio-state.edu/statistics/comp_exp/jour.club/MperkManual.pdf). Accessed: 2020-04-03.
- Heiser, W. J. and A. D’Ambrosio (2013). Clustering and prediction of rankings within a kemeny distance framework. In *Algorithms from and for Nature and Life*, pp. 19–31. Springer.
- IPCC (2018). Summary for policymakers. In: *Global Warming of 1.5°C. An IPCC Special Report on the impacts of global warming of 1.5°C above pre-industrial levels and related global greenhouse gas emission pathways, in the context of strengthening the global response to the threat of climate change, sustainable development, and efforts to eradicate poverty*, World Meteorological Organization, Geneva, Switzerland. [Masson-Delmotte, V., P. Zhai, H.-O. Pörtner, D. Roberts, J. Skea, P.R. Shukla, A. Pirani, W. Moufouma-Okia, C. Péan, R. Pidcock, S. Connors, J.B.R. Matthews, Y. Chen, X. Zhou, M.I. Gomis, E. Lonnoy, T. Maycock, M. Tignor, and T. Waterfield (eds.)].

- Kemeny, J. G. and L. Snell (1962). Preference ranking: an axiomatic approach. *Mathematical models in the social sciences*, 9–23.
- Kendall, M. G. (1948). Rank correlation methods.
- Kucherenko, S., S. Tarantola, and P. Annoni (2012). Estimation of global sensitivity indices for models with dependent variables. *Computer physics communications* 183(4), 937–946.
- Kuo, F. and S. Joe (2017). *SobolSequence: Sobol Sequences with Better Two-Dimensional Projections*. R package version 1.0.
- Linero, A. R. (2018). Bayesian regression trees for high-dimensional prediction and variable selection. *Journal of the American Statistical Association* 113(522), 626–636.
- Liu, Y., V. Ročková, and Y. Wang (2018). Abc variable selection with bayesian forests. *arXiv preprint arXiv:1806.02304*.
- Mara, T. A. and S. Tarantola (2012). Variance-based sensitivity indices for models with dependent inputs. *Reliability Engineering & System Safety* 107, 115–121.
- MATLAB (2017). *9.2.0.538062 (R2017a)*. Natick, Massachusetts: The MathWorks Inc.
- McCulloch, R., R. Sparapani, R. Gramacy, C. Spanbauer, and M. Pratola (2019). *BART: Bayesian Additive Regression Trees*. R package version 2.6.
- R Core Team (2018). *R: A Language and Environment for Statistical Computing*. Vienna, Austria: R Foundation for Statistical Computing.
- Saltelli, A., K. Chan, M. Scott, et al. (2000). *Sensitivity analysis. Probability and statistics series*.
- Saltelli, A. and I. M. Sobol’ (1995). About the use of rank transformation in sensitivity analysis of model output. *Reliability Engineering & System Safety* 50(3), 225 – 239.
- Santner, T. J., B. J. Williams, and W. I. Notz (2018). *The Design and Analysis of Computer Experiments, Second Edition*. Springer-Verlag.
- Sobol’, I. M. (1993). Sensitivity estimates for nonlinear mathematical models. *MMCE* 1(4), 407–414.
- UNFCCC (2015). Adoption of the paris agreement.
- Wickham, H. (2017). *tidyverse: Easily Install and Load the 'Tidyverse'*. R package version 1.2.1.



## 7 Appendix

*Proof of Theorem 1.* According to Equation 10, the first step to computing the Sobol' index for tree function  $g(\cdot; \mathcal{T}, \mathcal{M})$  and variable index set  $P \subset \{1, 2, \dots, d\}$  is to compute the conditional expectation  $\mathbb{E}_{\mathbf{X}_{-P}}[g(\mathbf{X}; \mathcal{T}, \mathcal{M}) \mid \mathbf{X}_P]$ . By taking the appropriate conditional expectation of both sides of Equation 3, we get

$$\mathbb{E}_{\mathbf{X}_{-P}}[g(\mathbf{X}; \mathcal{T}, \mathcal{M}) \mid \mathbf{X}_P] = \sum_{k=1}^{|\mathcal{M}|} d_k^{-P} \mathbf{1}_{\mathbf{R}_k^P}(\mathbf{X}_P), \quad (17)$$

where hyperrectangle  $\mathbf{R}_k^P = \prod_{i \in P} I_k^i$ , and coefficients  $d_k^{-P} = \mu_k \mathbb{P}_{-P}(\mathbf{R}_k^{-P})$ . Due to Assumption **A.1**, the coefficient expression simplifies to

$$d_k^{-P} = \mu_k \prod_{j \notin P} \mathbb{P}_j(I_k^j). \quad (18)$$

According to Equation 10, the first step to computing the Sobol' index for ensemble function  $\mathcal{E}(\cdot)$  and variable index set  $P \subset \{1, 2, \dots, d\}$  is to compute the conditional expectation  $\mathbb{E}_{\mathbf{X}_{-P}}[\mathcal{E}(\mathbf{X}) \mid \mathbf{X}_P]$ . By taking the appropriate conditional expectation of both sides of Equation 4, using linearity of expectations, and plugging in Equation 17, we get

$$\begin{aligned} \mathbb{E}_{\mathbf{X}_{-P}}[\mathcal{E}(\mathbf{X}) \mid \mathbf{X}_P] &= \sum_{t=1}^m \mathbb{E}_{\mathbf{X}_{-P}}[g(\mathbf{X}; \mathcal{T}_t, \mathcal{M}_t) \mid \mathbf{X}_P] \\ &= \sum_{t=1}^m \sum_{k=1}^{|\mathcal{M}_t|} d_{tk}^P \mathbf{1}_{\mathbf{R}_{tk}^P}(\mathbf{X}_P). \end{aligned}$$

It is more convenient to view this conditional expectation as a single sum over the ensemble's terminal nodes rather than as a double sum as shown above. Hence, we can express this conditional expectation as

$$\mathbb{E}_{\mathbf{X}_{-P}}[\mathcal{E}(\mathbf{X}) \mid \mathbf{X}_P] = \sum_{k \in B_{\mathcal{E}}} d_k^{-P} \mathbf{1}_{\mathbf{R}_k^P}(\mathbf{X}_P), \quad (19)$$

where  $B_{\mathcal{E}} = \cup_{t=1}^m B_{\mathcal{T}_t}$  is the index set over the terminal nodes of the trees in ensemble  $\mathcal{E}$ .

Finally we are able to compute the variance terms in Equation 10 for general variable index set  $P \subset \{1, 2, \dots, d\}$ . First, we compute  $\text{Var}_{\mathbf{X}_P} \left( \mathbb{E}_{\mathbf{X}_{-P}}[\mathcal{E}(\mathbf{X}) \mid \mathbf{X}_P] \right)$ . Into this term we plug in Equation 19, apply the general result  $\text{Var}(U) = \text{Cov}(U, U)$  for generic random variable  $U$ , and use the bilinearity property of covariance to get

$$\text{Var}_{\mathbf{X}_P} \left( \mathbb{E}_{\mathbf{X}_{-P}}[\mathcal{E}(\mathbf{X}) \mid \mathbf{X}_P] \right) = \sum_{k \in B_{\mathcal{E}}} \sum_{l \in B_{\mathcal{E}}} d_k^{-P} d_l^{-P} \text{Cov}_{\mathbf{X}_P} \left( \mathbf{1}_{\mathbf{R}_k^P}(\mathbf{X}_P), \mathbf{1}_{\mathbf{R}_l^P}(\mathbf{X}_P) \right),$$

where the coefficients  $d_k^{-P}$  and  $d_l^{-P}$  are defined in Equation 18. To each covariance term, which we will denote as  $C_{k,l}^P$ , we can apply the elementary covariance result  $\text{Cov}(U, V) = \mathbb{E}UV - \mathbb{E}U\mathbb{E}V$  for generic

random variables  $U$  and  $V$  to get

$$C_{k,l}^P = \mathbb{P}_P(\mathbf{R}_k^P \cap \mathbf{R}_l^P) - \mathbb{P}_P(\mathbf{R}_k^P)\mathbb{P}_P(\mathbf{R}_l^P). \quad (20)$$

Thus,

$$\text{Var}_{\mathbf{X}_P} \left( \mathbb{E}_{\mathbf{X}_{-P}}[\mathcal{E}(\mathbf{X}) \mid \mathbf{X}_P] \right) = \sum_{k \in B_{\mathcal{E}}} \sum_{l \in B_{\mathcal{E}}} d_k^{-P} d_l^{-P} C_{k,l}^P. \quad (21)$$

In particular, when  $P = \{i\}$ , then

$$\mathbb{E}_{\mathbf{X}_{-i}}[\mathcal{E}(\mathbf{X}) \mid X_i] = \sum_{k \in B_{\mathcal{E}}} d_k^{-i} \mathbf{1}_{I_k^i}(X_i), \quad (22)$$

where  $d_k^{-i} = \mu_k \prod_{j \neq i} \mathbb{P}_j(I_k^j)$ . The main-effects Sobol' index in Equation 10 then becomes

$$V_i = \sum_{k \in B_{\mathcal{E}}} \sum_{l \in B_{\mathcal{E}}} d_k^{-i} d_l^{-i} C_{k,l}^i, \quad (23)$$

where

$$C_{k,l}^i = \mathbb{P}_i(I_k^i \cap I_l^i) - \mathbb{P}_i(I_k^i)\mathbb{P}_i(I_l^i). \quad (24)$$

□

*Proof of Theorem 2.* Consider a BART ensemble  $\mathcal{E}_0$  with  $m$  regression trees, where each tree is simply a terminal node with one terminal node parameter. Thus, the ensemble  $\mathcal{E}_0$  predicts the same value for any input  $\mathbf{x} \in D$  and is hence a constant-mean model. Then any BART ensemble  $\mathcal{E}$  with  $m$  regression trees can be thought of as  $\mathcal{E}_0$  having undergone a sequence of birth processes. Any birth process slices a terminal node's corresponding hyperrectangle into two smaller hyperrectangles according to some split rule. If the call this split rule " $x_i < c$ ", then this slice occurs on the  $(p-1)$ -dimensional hyperplane  $x_i = c$  in  $D$ . The resulting "left" hyperrectangle gains a terminal node parameter  $\mu_{left}$  while the resulting "right" hyperrectangle gains a terminal node parameter  $\mu_{right}$ . Thus, if prior to the birth process the piecewise-constant function  $\mathbb{E}_{\mathbf{X}_{-i}}[\mathcal{E}(\mathbf{X}) \mid X_i = \cdot]$  is constant at  $x_i = c$  (which we ensure through assumption **A.3**) and  $\mu_{left} \neq \mu_{right}$  (which is true almost surely but is also ensured through assumption **A.4**), then the birth process produces a jump in the piecewise-constant function at  $x_i = c$ . Meanwhile, the birth process does not produce a jump in any of the other piecewise-constant functions  $\mathbb{E}_{\mathbf{X}_{-j}}[\mathcal{E}(\mathbf{X}) \mid X_j = \cdot]$  (for  $j \neq i$ ). Hence, under the mentioned conditions, each birth process that splits on variable  $x_i$  increments the number of jumps in the piecewise-constant function  $\mathbb{E}_{\mathbf{X}_{-i}}[\mathcal{E}(\mathbf{X}) \mid X_i = \cdot]$  by one. □

*Proof of Theorem 3.* We have the following transformations to the conditional expectation function  $\mathbb{E}_{\mathbf{X}_{-i}}[\mathcal{E}(\mathbf{X}) \mid X_i = \cdot]$ :

1. First, center and scale the  $e_{k^*}^i$ . Let

$$\tilde{e}_{k^*}^i = \sqrt{|B_{\mathcal{E}}^i|} \frac{e_{k^*}^i - \bar{e}_{\cdot}^i}{s},$$

where  $\bar{e}_{\cdot}^i = |B_{\mathcal{E}}^i|^{-1} \sum_{k^* \in B_{\mathcal{E}}^i} e_{k^*}^i$  and  $s^2 = [\sum_{k^* \in B_{\mathcal{E}}^i} (e_{k^*}^i - \bar{e}_{\cdot}^i)^2] / (|B_{\mathcal{E}}^i| - 1)$  is the corrected sample variance of the  $\{e_{k^*}^i\}$ .

2. Second, assign equal probability mass  $|B_{\mathcal{E}}^i|^{-1}$  to each  $I_{k^*}^i$ . Introduce new intervals  $\tilde{I}_{k^*}^i$  by shifting and scaling  $I_{k^*}^i$  so that

- (a)  $\{\tilde{I}_{k^*}^i\}_{k^* \in B_{\mathcal{E}}^i}$  still partitions  $I_D^i$  into exactly  $|B_{\mathcal{E}}^i|$  sets, and
- (b)  $\mathbb{P}_i(\tilde{I}_{k^*}^i) = |B_{\mathcal{E}}^i|^{-1}$  for all  $k^* \in B_{\mathcal{E}}^i$ .

Now define  $\tilde{\mathbb{E}}_{\mathbf{X}_{-i}}[\mathcal{E}(\mathbf{X}) \mid X_i = \cdot] := \sum_{k^* \in B_{\mathcal{E}}^i} \tilde{e}_{k^*}^i \mathbf{1}_{\tilde{I}_{k^*}^i}(\cdot)$ . Using previous definitions, we have

$$\begin{aligned} \text{Var}_{X_i}(h_{\mathcal{E}}^i(X_i)) &= \text{Var}_{X_i}\left(\sum_{k^* \in B_{\mathcal{E}}^i} \tilde{e}_{k^*}^i \mathbf{1}_{\tilde{I}_{k^*}^i}(X_i)\right) \\ &= \sum_{k^* \in B_{\mathcal{E}}^i} \sum_{l^* \in B_{\mathcal{E}}^i} \tilde{e}_{k^*}^i \tilde{e}_{l^*}^i \left[ \mathbb{P}_i(\tilde{I}_{k^*}^i \cap \tilde{I}_{l^*}^i) - \mathbb{P}_i(\tilde{I}_{k^*}^i) \mathbb{P}_i(\tilde{I}_{l^*}^i) \right]. \end{aligned}$$

Recall that the intervals  $\tilde{I}_{k^*}^i$  still partition the original domain  $I_D^i$ . So if  $k^* \neq l^*$ , then  $\tilde{I}_{k^*}^i \cap \tilde{I}_{l^*}^i = \emptyset$  and hence  $\mathbb{P}_i(\tilde{I}_{k^*}^i \cap \tilde{I}_{l^*}^i) = 0$ . Thus,

$$\sum_{k^* \in B_{\mathcal{E}}^i} \sum_{l^* \in B_{\mathcal{E}}^i} \tilde{e}_{k^*}^i \tilde{e}_{l^*}^i \mathbb{P}_i(\tilde{I}_{k^*}^i \cap \tilde{I}_{l^*}^i) = \sum_{k^* \in B_{\mathcal{E}}^i} (\tilde{e}_{k^*}^i)^2 \mathbb{P}_i(\tilde{I}_{k^*}^i).$$

Since each interval  $\tilde{I}_{k^*}^i$  has equal probability mass, each  $\mathbb{P}_i(\tilde{I}_{k^*}^i)$  becomes simply  $|B_{\mathcal{E}}^i|^{-1}$ . So then

$$\text{Var}_{X_i}(h_{\mathcal{E}}^i(X_i)) = |B_{\mathcal{E}}^i|^{-1} \sum_{k^* \in B_{\mathcal{E}}^i} (\tilde{e}_{k^*}^i)^2 - |B_{\mathcal{E}}^i|^{-2} \sum_{k^* \in B_{\mathcal{E}}^i} \sum_{l^* \in B_{\mathcal{E}}^i} \tilde{e}_{k^*}^i \tilde{e}_{l^*}^i.$$

Note that the coefficients  $\tilde{e}_{k^*}^i$  are centered so that the sum  $\sum_{k^* \in B_{\mathcal{E}}^i} \tilde{e}_{k^*}^i$  (and hence the double sum term in the preceding equation) equals zero. Also note that the  $\tilde{e}_{k^*}^i$  are scaled so that  $\sum_{k^* \in B_{\mathcal{E}}^i} (\tilde{e}_{k^*}^i)^2 = |B_{\mathcal{E}}^i|(|B_{\mathcal{E}}^i| - 1)$ . We then have

$$\text{Var}_{X_i}(h_{\mathcal{E}}^i(X_i)) = |B_{\mathcal{E}}^i| - 1.$$

Recall that the set  $B_{\mathcal{E}}^i$  indexes the set of intervals  $I_{k^*}^i = [\gamma_1, \gamma_2)$  (or  $[\gamma_1, \gamma_2]$  if  $\gamma_2 = b_D^i$ ), where  $\gamma_1$  and  $\gamma_2$  are any two consecutive (in value) points in  $\bar{C}_{\mathcal{E}}^i$ . Thus, the number of such intervals  $I_{k^*}^i$  is one less than the number of values in  $\bar{C}_{\mathcal{E}}^i = C_{\mathcal{E}}^i \cup \{a_D^i, b_D^i\}$ . That is, the value  $\text{Var}_{X_i}(h_{\mathcal{E}}^i(X_i)) = |B_{\mathcal{E}}^i| - 1 = (|\bar{C}_{\mathcal{E}}^i| - 1) - 1 = |C_{\mathcal{E}}^i|$ , which, due to assumption A4, equals the number of nodes in  $\mathcal{E}$  that splits on variable  $X_i$ , which, for almost all values of  $\mathcal{M} \mid \mathcal{T}$  parameters in  $\mathcal{E}$ , equals the number of jumps in  $h_{\mathcal{E}}^i(x_i)$ . Thus,  $\text{Var}_{X_i}(h_{\mathcal{E}}^i(X_i))$  for almost all values of  $\mathcal{M} \mid \mathcal{T}$  parameters in  $\mathcal{E}$  equals the number of jumps in  $h_{\mathcal{E}}^i$ .  $\square$

*Proof of Theorem 4.* For any terminal node  $k \in B_{\mathcal{E}}$  where  $v(k) \cap P = \emptyset$ , the random quantity  $\mathbb{E}[\mu_k \mathbf{1}_{\mathbf{R}_k}(\mathbf{X}) \mid \mathbf{X}_P]$  is in fact constant. Therefore,

$$\begin{aligned} \text{Var}_{\mathbf{X}_P}(\mathbb{E}[\mathcal{E}(\mathbf{X}) - \mu_k \mathbf{1}_{\mathbf{R}_k}(\mathbf{X}) \mid \mathbf{X}_P]) &= \text{Var}_{\mathbf{X}_P}(\mathbb{E}[\mathcal{E}(\mathbf{X}) \mid \mathbf{X}_P] - \mathbb{E}[\mu_k \mathbf{1}_{\mathbf{R}_k}(\mathbf{X}) \mid \mathbf{X}_P]) \\ &= \text{Var}_{\mathbf{X}_P}(\mathbb{E}[\mathcal{E}(\mathbf{X}) \mid \mathbf{X}_P]). \end{aligned}$$

The result of the theorem will follow by applying this argument to all such terminal nodes.  $\square$

*Proof.* Proof of Theorem 5. In general, the Kemeny-Snell (KS) distance between rankings  $\alpha = (\alpha_1, \dots, \alpha_p)$  and  $\beta = (\beta_1, \dots, \beta_p)$  is defined to be

$$d_{KS}(\alpha, \beta) = \frac{1}{2} \sum_{i=1}^p \sum_{j=1}^p |A_{ij} - B_{ij}|$$

where

$$A_{ij} = \begin{cases} 1 & \alpha \text{ prefers object } i \text{ to object } j \\ -1 & \alpha \text{ prefers object } j \text{ to object } i \\ 0 & \alpha \text{ prefers objects } i \text{ and } j \text{ equally} \end{cases}$$

and  $B_{ij}$  is similarly defined for ranking  $\beta$ .

For the rest of the proof, we will assume that rankings  $\alpha$  and  $\beta$  each have no ties. We will also take ranking  $\alpha$  to be the reference vector and hence will, without loss of generality, assume  $\alpha = (1, 2, \dots, p)$ . We will also refer to the sum in Equation 16 as the discrepancy  $d_r$ . Finally, we will prove desired equality via induction.

We first note that these assumptions greatly simplify the KS distance. If we think of the values  $A_{ij}$  (similarly  $B_{ij}$ ) as constituting a  $p \times p$  matrix  $A$  (similarly  $B$ ) whose  $ij$  entry is  $A_{ij}$  (similarly  $B_{ij}$ ), then both matrices  $A$  and  $B$  are antisymmetric, which implies  $|A_{ij} - B_{ij}| = |A_{ji} - B_{ji}|$  for all  $i, j = 1, \dots, p$  and  $A_{ij} = B_{ij} = 0$  if  $i = j$ . Therefore, we may reformulate the KS distance as

$$d_{KS}(\alpha, \beta) = \sum_{i < j} |A_{ij} - B_{ij}|.$$

We now proceed with the proof by induction. Suppose  $p = 2$ . Half the KS distance is then  $\frac{1}{2}|A_{12} - B_{12}|$ , where  $A_{12} = 1$ , while the AH distance becomes  $W_1$  (since  $W_p = 0$  by default). One of two cases may occur. If  $\beta_1 < \beta_2$ , then  $\beta_1 = 1$  and  $\beta_2 = 2$ . In this case, both the AH distance and half the KS distance are zero. If  $\beta_1 > \beta_2$ , then  $\beta_1 = 2$  and  $\beta_2 = 1$ . In this case, both the AH distance and half the KS distance are unity. We note that values  $\beta_1$  and  $\beta_2$  must be distinct due to ranking  $\beta$  having no ties. Thus, the induction hypothesis holds for  $p = 2$ .

Now suppose the induction hypothesis holds for arbitrary  $p-1 \geq 3$ . The KS distance can be decomposed into

$$d_{KS}(\alpha, \beta) = d_{KS}(\alpha_{-1}, \beta_{-1}) + \sum_{j=2}^p |A_{1j} - B_{1j}|,$$

where we define  $\alpha_{-1} := (\alpha_2, \dots, \alpha_p)$  and  $\beta_{-1}$  similarly for ranking  $\beta$ . The the discrepancy  $d_r$ , due to its stagewise nature, can also be decomposed:

$$d_{AH}(\alpha, \beta) = W_1 + d_{AH}(\alpha_{-1}, \beta_{-1}),$$

where  $W_1 = \beta_1 - 1$  by default. By assumption, half the KS distance between  $\alpha_{-1}$  and  $\beta_{-1}$  equals the discrepancy  $d_r$  between the same two quantities. Hence, we need only prove that  $\frac{1}{2} \sum_{j=2}^p |A_{1j} - B_{1j}| = \beta_1 - 1$  to complete the proof.

First, we note that  $A_{1j} = 1$  for all  $j > 1$  and, since  $B_{1j}$  is either 1 or  $-1$ , the quantity  $A_{1j} - B_{1j}$

is nonnegative. Thus,  $|A_{1j} - B_{1j}| = 1 - B_{1j}$  for all  $j > 1$ . But  $B_{1j}$  is simply  $\mathbf{1}_{\beta_1 < \beta_j} - \mathbf{1}_{\beta_1 > \beta_j}$ . Hence,  $\sum_{j=2}^p B_{1j} = (p - \beta_1) - (\beta_1 - 1) = p - 2\beta_1 + 1$ . Therefore,  $\frac{1}{2} \sum_{j=2}^p |A_{1j} - B_{1j}| = \beta_1 - 1$ .  $\square$

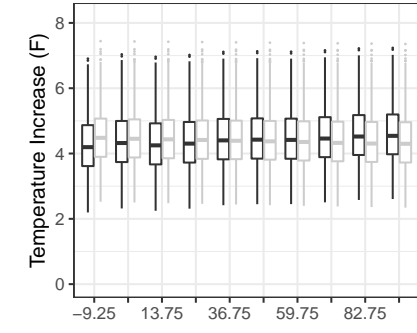
*Proof.* Proof of Theorem 6. Suppose we have computed discordances  $W_1, \dots, W_{k-1}$  for some  $k > q_0$  and wish to compute discordance  $W_k$ . Then the remaining considered items, each having input activity measure values of zero, all have ranking number 1 in ranking  $\rho_f$ . Since at least one remaining considered item has ranking number 1 in ranking  $\rho_{\mathcal{E}}$ , we get  $W_k = 1 - 1 = 0$ .  $\square$

*Proof.* Proof of Theorem 7. We will partition the discordances into three sets:  $\{W_1, \dots, W_{j-1}\}$ ,  $\{W_j, \dots, W_{j+u-1}\}$ , and  $\{W_{j+u}, \dots, W_{|\rho_f|}\}$ . After letting, for all  $k = 1, \dots, j-1, j+u, \dots, |\rho_f|$ , item  $i_k$  be the item removed from consideration after computing  $W_k$  but (if  $k < |\rho_f|$ ) before computing  $W_{k+1}$ , we will then prove the desired invariance to permutation  $\phi$  for the three sets of discordances.

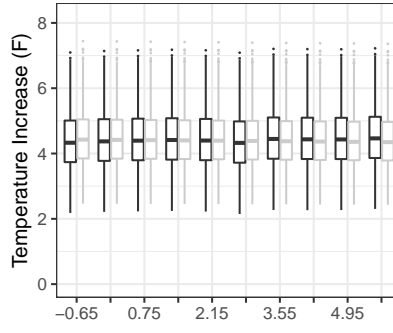
First, consider discordances  $W_1, \dots, W_{j-1}$ . These discordances depend only on the ranking numbers of items  $i_1, \dots, i_{j-1}$  in  $\rho_f$  and in  $\rho_{\mathcal{E}}$ . Because these ranking numbers are invariant to choice of permutation  $\phi$ , these discordances are also invariant to  $\phi$ .

Now consider discordances  $W_{j+u}, \dots, W_{|\rho_f|}$ . Similar to the previous set of discordances, these discordances depend only on the ranking numbers of items  $i_{j+u}, \dots, i_{|\rho_f|}$  in  $\rho_f$  and in  $\rho_{\mathcal{E}}$ . Because these ranking numbers are invariant to choice of permutation  $\phi$ , these discordances are also invariant to  $\phi$ .

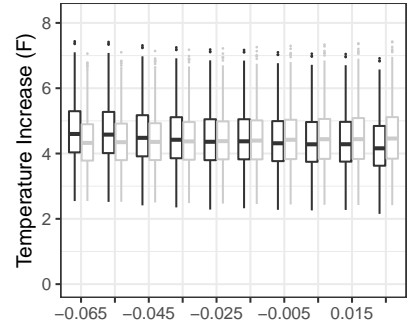
Finally, consider discordances  $W_j, \dots, W_{j+u-1}$ . Because items  $i_{j+1}, \dots, i_{j+u}$  (and no other items) have ranking number  $j$  in  $\rho_f$ , these discordance values are  $W_k = r_{(k)} - j + 1$  for  $k = j, \dots, j+u-1$ , where  $r_{(j)}, \dots, r_{(j+u-1)}$  are the order statistics of ranking numbers  $r_j, \dots, r_{j+u-1}$ . Because order statistics are invariant to permutations of the statistic values, these discordances are invariant to permutation  $\phi$ .  $\square$



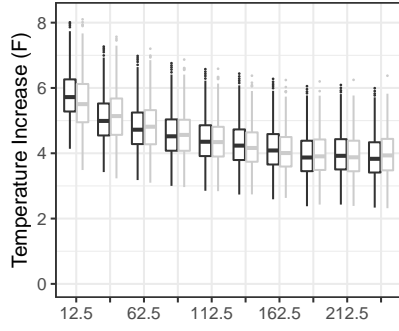
(a) Oil.



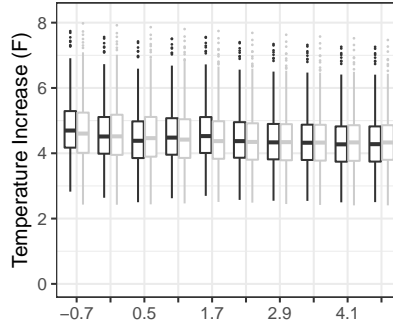
(b) Gas.



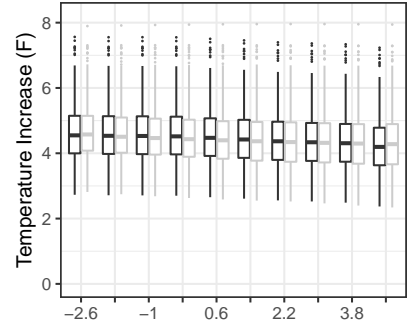
(c) Renewables.



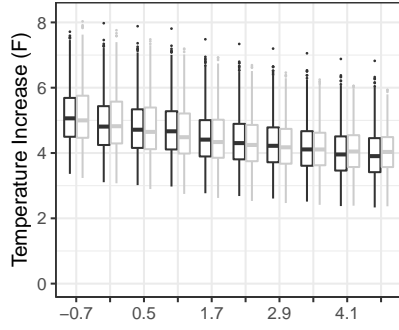
(d) Carbon Price.



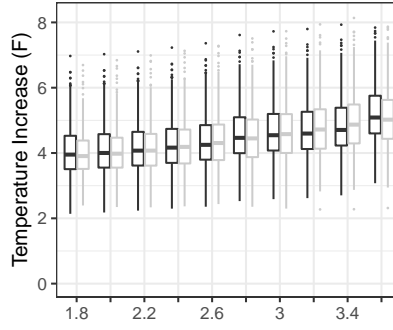
(e) Energy Efficiency (Transport).



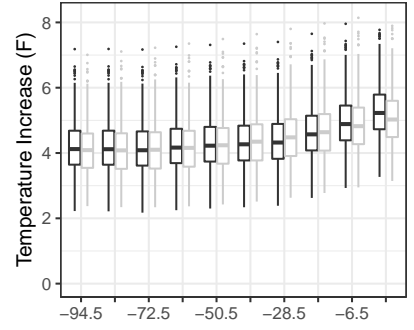
(f) Electrification (Transport).



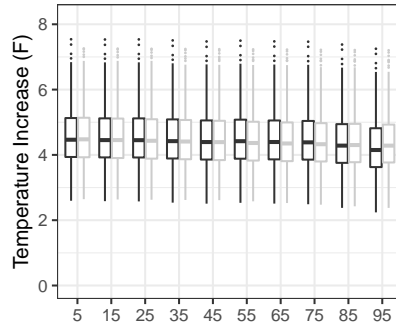
(g) Energy Efficiency (Buildings and Industry).



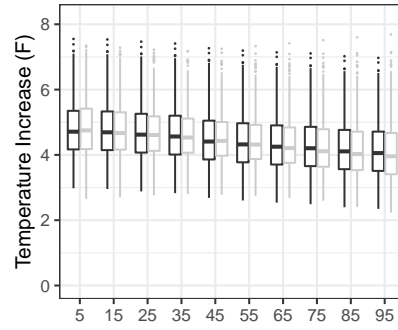
(h) Economic Growth.



(i) Methane & Other.



(j) Afforestation.



(k) Technological (Carbon Removal).

Figure 8: Range plots for each of the 11 input variables.